

# Gravitational waves from first-order electroweak phase transition in a model with light sgoldstinos

---

S. Demidov,<sup>a,b</sup> D. Gorbunov<sup>a,b</sup> and E. Kriukova<sup>a,c</sup>

<sup>a</sup>*Institute for Nuclear Research of the Russian Academy of Sciences,  
60th October Anniversary pr-ct 7a, Moscow 117312, Russia*

<sup>b</sup>*Landau Phystech School of Physics and Research, Moscow Institute of Physics and Technology,  
Institutskiy per. 9, Dolgoprudny 141700, Russia*

<sup>c</sup>*Faculty of Physics, Lomonosov Moscow State University,  
Leninskiye Gory 1-2, Moscow 119991, Russia*

*E-mail:* [demidov@inr.ac.ru](mailto:demidov@inr.ac.ru), [gorby@inr.ac.ru](mailto:gorby@inr.ac.ru),  
[kryukova.ea15@physics.msu.ru](mailto:kryukova.ea15@physics.msu.ru)

**ABSTRACT:** We study previously unexplored possibility of triggering the first order electroweak phase transition (EWPT) by interactions of the Standard Model (SM) particles with the sector responsible for low scale supersymmetry breaking. The low-energy theory apart from the SM particles contains additional scalar degrees of freedom — sgoldstinos — which contribute to the effective scalar potential and thus can trigger the first order EWPT. Remarkably, the latter requires only moderate couplings in the scalar sector. The perturbative description in terms of the effective theory seems formally to be applicable upto the scale of supersymmetry breaking: the Landau pole in the scalar sector is above  $10^8$ - $10^9$  GeV. We calculate the gravitational wave signal generated at this transition (it can be tested, e.g. by LISA, BBO and DECIGO) and briefly discuss the collider phenomenology of this scenario.

ARXIV EPRINT: [2112.06083](https://arxiv.org/abs/2112.06083)

---

## Contents

<b>1</b>	<b>Introduction</b>	<b>1</b>
<b>2</b>	<b>MSSM with goldstino supermultiplet</b>	<b>3</b>
<b>3</b>	<b>Effective potential of the model</b>	<b>5</b>
<b>4</b>	<b>Numerical results</b>	<b>11</b>
4.1	First-order electroweak phase transition	12
4.2	Gravitational waves	15
4.3	Relation to parameters of supersymmetric model	18
<b>5</b>	<b>Conclusions</b>	<b>22</b>
<b>A</b>	<b>One-loop renormalization group equations</b>	<b>22</b>

---

## 1 Introduction

There are plenty of well motivated new physics scenarios which were proposed to solve phenomenological problems of the Standard Model (SM), and supersymmetry [1, 2] is among the most attractive paradigms for the SM extension. Technically natural supersymmetric scenarios predict superpartners with masses near the electroweak scale. Yet, so far no signals from supersymmetry have been seen at LHC experiments [3, 4] except for several existing anomalies in the experimental data which are still inconclusive.

Surely, in a realistic supersymmetric scenario the supersymmetry must be broken. In the case of spontaneously broken supersymmetry the model should contain the sector which is responsible for this spontaneous supersymmetry breaking (SSB). In the framework of global supersymmetry the SSB implies existence of the Goldstone fermion, *goldstino* [5], which becomes the longitudinal component of gravitino in supergravity (local supersymmetry) extensions [6]. In a full model goldstino should be a member of supermultiplet from the hidden sector. It is phenomenologically possible that some of particles inhabiting this sector are lighter than superpartners of the SM particles and in some classes of models they may show up in experiments before the superpartners. One of such scenarios, which we consider in this study, is the models with low scale supersymmetry breaking that can appear in several

setups [7–10]. In the simplest case the low-energy part of the hidden sector in these models consists of a single chiral superfield

$$\Phi = \phi + \sqrt{2}\psi\theta + \theta\theta F_\Phi, \quad (1.1)$$

where  $\psi$  is goldstino,  $\phi = \frac{1}{\sqrt{2}}(s+ip)$  are its scalar superpartners, *sgoldstinos*, and  $F_\Phi$  is an auxiliary field which upon SSB gains non-zero vacuum expectation value  $\langle F_\Phi \rangle = F$  with  $\sqrt{F}$  being the energy scale of supersymmetry breaking. Within the low scale supersymmetry, it is assumed that this scale is not far from the electroweak scale. Correspondingly, the gravitino has the mass  $m_{3/2} \sim \frac{F}{M_{\text{Pl}}}$  and this state is the lightest supersymmetric particle. Sgoldstinos, on the other hand, acquire non-zero masses through interactions in the hidden sector (sgoldstinos are massless at the tree level of perturbation theory). In this study we consider the scenario with sgoldstinos at the electroweak (or subTeV) scale, while other superpartners are significantly heavier. General aspects of this setup were discussed in refs. [11, 12] and this scenario exhibits quite rich phenomenology, see, e.g. [13–21]. In particular, presence of relatively light sgoldstinos can noticeably affect the Higgs sector of the model, see e.g. [22–24].

Here we consider yet unexplored possibility that new light scalar degrees of freedom, from the sector where supersymmetry gets broken, contribute to the low-energy effective potential and can trigger the first order electroweak phase transition. In the decoupling regime the low-energy theory contains additional complex-valued scalar field whose coupling constants to the SM fields are determined mainly by ratios of soft supersymmetry breaking parameters to the supersymmetry breaking scale squared. Possibility of the first order EWPT in the SM extensions with new scalars was studied in literature, see e.g. refs. [25–32]. The interest to the first order EWPT is associated with possible realisation of the electroweak baryogenesis [33, 34] and generation of observable gravitational wave signal [35–39]. In this study we concentrate on the latter option. The gravitational wave signal from the first-order phase transition due to SUSY breaking in the hidden sector was previously studied in [40]. We, however, scrutinize on possible influence of the sector responsible for SUSY breaking on EWPT.

We study a part of the parameter space of supersymmetric model with light sgoldstinos which admits the first order EWPT in the early Universe. Naturally it is provided by interactions between the new ingredients in the scalar sector and the SM Higgs field. Typically, for the first order EWPT to take place, the corresponding couplings must be rather large, see model examples in the references above, which exhibit Landau poles not far from the electroweak scale. It requires new physics there and rises the question of whether the description of the EWPT in terms of the effective low-energy theory is fully justified. In our case the couplings in the scalar sectors turn out to be rather moderate, and the corresponding Landau poles lifted up to the energy scale as high as  $10^8$ - $10^9$  GeV. Therefore one can formally use the effective description of this model upto this scale where it is completed by

introducing new particles: those responsible for the supersymmetry breaking in the hidden sector, those responsible for the mediation of the supersymmetry breaking to the visible (SM) sectors, the SM superpartners etc. Evidently, the supersymmetry breaking scale may be well lower, moreover, one can expect the SM superpartners mass scale to be lower, and so the model is modified at the lower scale of their masses. In any case the effective description works in the fairly wide energy region allowing for a broad class of supersymmetric models to complete it at high energies. Therefore, applying the effective model description we calculate the gravitational wave signal that can be observed at LISA and proposed experiments BBO, DECIGO and Ultimate DECIGO [41]. We also discuss a promising collider phenomenology pertinent to this scenario.

The rest of the paper is organised as follows. In Section 2 we introduce the supersymmetric model with low-energy goldstino supermultiplet. Section 3 describes the effective potential of low-energy model (including one-loop and thermal corrections) and spectrum of its scalar sector. In Section 4 we present numerical results on possibility of the first order EWPT and calculate spectrum of gravitational waves generated during this transition. Section 5 is left for conclusions and discussion.

## 2 MSSM with goldstino supermultiplet

We consider a supersymmetric model in which the Lagrangian of Minimal Supersymmetric Standard Model (MSSM) is extended by interactions involving goldstino superfield  $\Phi$ . Since the auxiliary field  $F_\Phi$  of goldstino multiplet acquires non-zero vev  $F$  upon SSB, the interaction of  $\Phi$  with MSSM fields yields soft supersymmetry breaking terms. The Lagrangian of the model can be written as a sum (see, e.g. [42])

$$\mathcal{L} = \mathcal{L}_K + \mathcal{L}_W + \mathcal{L}_{\text{gauge}} + \mathcal{L}_\Phi, \quad (2.1)$$

where the terms involving Kähler potential  $\mathcal{L}_K$  read

$$\mathcal{L}_K = \int d^2\theta d^2\bar{\theta} \sum_k \left( 1 - \frac{m_k^2}{F^2} \Phi^\dagger \Phi \right) \Phi_k^\dagger e^{g_1 V_1 + g_2 V_2 + g_3 V_3} \Phi_k, \quad (2.2)$$

here the sum is taken over all chiral matter superfields  $\Phi_k$ ,  $m_k$  are soft masses,  $g_k$  and  $V_k$  are the coupling constants and vector superfields of the  $U(1)_Y$ ,  $SU(2)_W$ ,  $SU(3)_c$  gauge groups. The part of the Lagrangian  $\mathcal{L}_W$  coming from superpotential of the model has the form

$$\begin{aligned} \mathcal{L}_W = \int d^2\theta \epsilon_{ij} & \left( \left( \mu - \frac{B}{F} \Phi \right) H_d^i H_u^j + \left( Y_{ab}^L + \frac{A_{ab}^L}{F} \Phi \right) L_a^j E_b^c H_d^i + \right. \\ & \left. + \left( Y_{ab}^D + \frac{A_{ab}^D}{F} \Phi \right) Q_a^j D_b^c H_d^i + \left( Y_{ab}^U + \frac{A_{ab}^U}{F} \Phi \right) Q_a^i U_b^c H_u^j \right) + h.c., \quad (2.3) \end{aligned}$$

here  $\mu$  is the higgsino mixing parameter,  $L, E$  are the left and right lepton superfields,  $Q, U, D$  are superfields of left, right up and down quarks,  $H_u, H_d$  are the Higgs doublet superfields,  $Y_{ab}^{L,D,U}$  are the Yukawa matrices,  $A_{ab}^L, A_{ab}^D, A_{ab}^U$  are soft trilinear constants;  $a, b = 1, 2, 3$  and superscript 'c' refers to the charged conjugated quantities. The Lagrangian involving gauge vector superfields  $\mathcal{L}_{\text{gauge}}$  is

$$\mathcal{L}_{\text{gauge}} = \frac{1}{4} \sum_a \int d^2\theta \left( 1 + \frac{2M_a}{F} \Phi \right) \text{Tr} W_{a\alpha} W_a^\alpha + h.c. , \quad (2.4)$$

where the sum goes over all the gauge groups of SM ( $a = 1, 2, 3$  for  $U(1)_Y, SU(2)_W, SU(3)_c$ ), while  $M_1, M_2, M_3$  stand for the corresponding gaugino masses.

When  $\Phi$  (1.1) with  $\langle F_\Phi \rangle = F$  is substituted into eqs. (2.2)–(2.4), the terms proportional to  $\Phi$  (and their Hermitian conjugates) in (2.3) and (2.4) provide soft trilinear terms and gaugino masses, while terms in (2.2) proportional to  $\Phi^\dagger \Phi$  yield soft masses squared for the model scalars, i.e. Higgs bosons and superpartners of the SM fermions. These terms also induce goldstino couplings to the SM particles and their superpartners; we ignore the latter in our study, concentrating on the models where the superpartners are very heavy. Finally, these terms give rise to sgoldstino couplings to the SM particles which we include in our study.

Then we introduce the Lagrangian of sgoldstino multiplet

$$\begin{aligned} \mathcal{L}_\Phi = \int d^2\theta d^2\bar{\theta} & \left( \Phi^\dagger \Phi - \frac{\widetilde{m}_s^2 + \widetilde{m}_p^2}{8F^2} (\Phi^\dagger \Phi)^2 - \frac{\widetilde{m}_s^2 - \widetilde{m}_p^2}{12F^2} (\Phi^\dagger \Phi^3 + \Phi^{\dagger 3} \Phi) - \right. \\ & - \frac{\delta_{\lambda_2}}{4F^2} H_u^\dagger H_u (\Phi^\dagger \Phi)^2 - \frac{\delta_{\lambda_3}}{9F^2} (\Phi^\dagger \Phi)^3 - \frac{\delta_{\lambda_4}}{3F^2} H_u^\dagger H_u (\Phi^\dagger \Phi^3 + \Phi^{\dagger 3} \Phi) - \\ & - \frac{\delta_{\lambda_5}}{5F^2} (\Phi^\dagger \Phi^5 + \Phi^{\dagger 5} \Phi) - \frac{\delta_{\lambda_6}}{8F^2} (\Phi^{\dagger 2} \Phi^4 + \Phi^{\dagger 4} \Phi^2) - \frac{\delta_{\mu_1}}{2F^2} H_u^\dagger H_u (\Phi^\dagger \Phi^2 + \Phi^{\dagger 2} \Phi) - \\ & \left. - \frac{\delta_{\mu_2}}{6F^2} (\Phi^{\dagger 3} \Phi^2 + \Phi^{\dagger 2} \Phi^3) - \frac{\delta_{\mu_3}}{4F^2} (\Phi^{\dagger 4} \Phi + \Phi^{\dagger} \Phi^4) - \frac{\delta_{C_3}}{2F^2} (\Phi^{\dagger 2} \Phi + \Phi^{\dagger} \Phi^2) \right) - \\ & - \left( \int d^2\theta F \Phi + h.c. \right). \quad (2.5) \end{aligned}$$

Here  $\widetilde{m}_s^2$  and  $\widetilde{m}_p^2$  are the mass parameters of scalar and pseudoscalar sgoldstinos, which become explicit upon substituting (1.1) with  $\langle F_\Phi \rangle = F$ .

We note in passing that the MSSM soft parameters as well as other new model parameters entering (2.5) can be generically complex-valued. In the present study we do not discuss CP-violation and assume all the relevant parameters to be real. Also, the described setup should be considered as a low-energy effective theory valid at energies below  $\sqrt{F}$ . It is in the perturbative regime as far as all the soft supersymmetry breaking terms are smaller than  $\sqrt{F}$ .

Most studies of the goldstino supermultiplet phenomenology limit themselves to the first three terms in (2.5) and the very last one triggering SSB in the model. Here

we add new set of higher dimensional operators with couplings constants of the same order  $\frac{1}{F^2}$  as the second and third terms in (2.5). Therefore, they may emerge in the same way, e.g. technically upon integrating out all the heavy fields in the hidden sector. Parameters  $\delta_{\lambda_i}$ ,  $i = 2, \dots, 6$  are dimensionless, parameters  $\delta_{\mu_i}$ ,  $i = 1, 2$  have dimension of mass, while  $\delta_{C_3}$  has dimension of squared mass. We will discuss their role in due course.

### 3 Effective potential of the model

In what follows we are going to study the electroweak phase transition in the early Universe within this model. Properties of the EWPT are determined by the effective potential at the non-zero finite temperature. This potential can be calculated by making use of different approaches. In our study we use the perturbation theory and calculate the one-loop effective potential including finite temperature corrections.

The tree-level scalar potential of the model is

$$V = V_{11} + V_{12} + V_{21} + V_{22}, \quad (3.1)$$

$$V_{11} = \frac{g_1^2}{8} \left( 1 + \frac{M_1}{F}(\phi + \phi^*) \right)^{-1} \left[ h_d^\dagger h_d - h_u^\dagger h_u - \frac{\phi^* \phi}{F^2} \left( m_d^2 h_d^\dagger h_d - m_u^2 h_u^\dagger h_u \right) \right]^2, \quad (3.2)$$

$$V_{12} = \frac{g_2^2}{8} \left( 1 + \frac{M_2}{F}(\phi + \phi^*) \right)^{-1} \left[ h_d^\dagger \sigma_a h_d + h_u^\dagger \sigma_a h_u - \frac{\phi^* \phi}{F^2} \left( m_d^2 h_d^\dagger \sigma_a h_d + m_u^2 h_u^\dagger \sigma_a h_u \right) \right]^2, \quad (3.3)$$

$$\begin{aligned} V_{21} = & \left( 1 - \frac{\widetilde{m}_s^2 + \widetilde{m}_p^2}{2F^2} \phi^* \phi - \frac{\widetilde{m}_s^2 - \widetilde{m}_p^2}{4F^2} (\phi^2 + \phi^{*2}) - \frac{m_u^2}{F^2} h_u^\dagger h_u - \frac{m_d^2}{F^2} h_d^\dagger h_d - \right. \\ & - \frac{m_u^4}{F^4} h_u^\dagger h_u \phi^* \phi - \frac{m_d^4}{F^4} h_d^\dagger h_d \phi^* \phi - \frac{\delta_{\lambda_2}}{F^2} h_u^\dagger h_u \phi^* \phi - \frac{\delta_{\lambda_3}}{F^2} (\phi^* \phi)^2 - \frac{\delta_{\lambda_4}}{F^2} h_u^\dagger h_u (\phi^2 + \phi^{*2}) - \\ & - \frac{\delta_{\lambda_5}}{F^2} (\phi^4 + \phi^{*4}) - \frac{\delta_{\lambda_6}}{F^2} \phi^* \phi (\phi^2 + \phi^{*2}) - \frac{\delta_{\mu_1}}{F^2} h_u^\dagger h_u (\phi + \phi^*) - \frac{\delta_{\mu_2}}{F^2} \phi^* \phi (\phi + \phi^*) - \\ & \left. - \frac{\delta_{\mu_3}}{F^2} (\phi^3 + \phi^{*3}) - \frac{\delta_{C_3}}{F^2} (\phi + \phi^*) \right)^{-1} \times \left| F + (-h_d^0 h_u^0 + H^- H^+) \times \right. \\ & \left. \times \left( \frac{B}{F} - \frac{m_u^2 + m_d^2}{F^2} \phi^* \left( \mu - \frac{B}{F} \phi \right) - \frac{\delta_{\mu_1}}{2F^2} \phi^* (2\phi + \phi^*) \mu \right) \right|^2, \quad (3.4) \end{aligned}$$

$$V_{22} = \frac{\mu^2 \phi \phi^*}{F^2} \left( m_u^2 h_d^\dagger h_d + m_d^2 h_u^\dagger h_u \right) + \left| \mu - \frac{B}{F} \phi \right|^2 \left( h_d^\dagger h_d + h_u^\dagger h_u \right). \quad (3.5)$$

Here  $h_d = \begin{pmatrix} h_d^0 \\ H^- \end{pmatrix}$ ,  $h_u = \begin{pmatrix} H^+ \\ h_u^0 \end{pmatrix}$  are the Higgs doublets. The above expressions agree with the potential found in [24] if one puts all the ' $\delta$ '-couplings entering (2.5) to zero. Note that in the Lagrangian each power of sgoldstino field comes with the

power of  $1/F$ , therefore for  $\sqrt{F}$  to be considerably larger than sgoldstino masses and soft SUSY breaking parameters the higher order interaction terms are parametrically suppressed; consequently, in (3.1)–(3.5) we neglect all the terms suppressed by  $1/F^3$  and stronger. For the same reason, in this work we limit ourselves to interactions of the Higgs doublets to sgoldstino up to the second power in the latter.

In this study we consider a scenario where all superpartners of the SM particles are considerably heavier than sgoldstinos, which are assumed to have masses of the order of the electroweak scale. For the Higgs sector it corresponds to the decoupling regime of MSSM. At low energies we are left with a single Higgs doublet  $\mathcal{H}$  instead of  $h_u$  and  $h_d$ : all the MSSM Higgs bosons are heavy except for the SM-like Higgs field. The low-energy effective Lagrangian can be obtained via the following substitution

$$h_u \rightarrow \mathcal{H} \sin \beta, \quad h_d \rightarrow -\epsilon \mathcal{H}^* \cos \beta. \quad (3.6)$$

Here  $\tan \beta = v_u/v_d$  with  $v_u$  and  $v_d$  being vacuum expectation values of neutral components of the Higgs doublets,  $h_u$  and  $h_d$ , respectively. The tree-level potential at zero temperature can be written in terms of the Higgs doublet  $\mathcal{H}$  and the complex scalar sgoldstino field  $\phi$  as

$$V_{\text{tree}}(\mathcal{H}, \phi) = V_{\text{quartic}}(\mathcal{H}, \phi) + V_{\text{cubic}}(\mathcal{H}, \phi) + V_{\text{free}}(\mathcal{H}, \phi), \quad (3.7)$$

where

$$V_{\text{quartic}}(\mathcal{H}, \phi) = \lambda_1(\mathcal{H}^\dagger \mathcal{H})^2 + \lambda_2 \phi^* \phi \mathcal{H}^\dagger \mathcal{H} + \lambda_3(\phi^* \phi)^2 + \lambda_4(\phi^2 + \phi^{*2})\mathcal{H}^\dagger \mathcal{H} + \lambda_5(\phi^4 + \phi^{*4}) + \lambda_6 \phi^* \phi (\phi^2 + \phi^{*2}), \quad (3.8)$$

$$V_{\text{cubic}}(\mathcal{H}, \phi) = \frac{\mu_1}{\sqrt{2}}(\phi + \phi^*)\mathcal{H}^\dagger \mathcal{H} + \frac{\mu_2}{\sqrt{2}}(\phi + \phi^*)\phi^* \phi + \frac{\mu_3}{\sqrt{2}}(\phi^3 + \phi^{*3}), \quad (3.9)$$

$$V_{\text{free}}(\mathcal{H}, \phi) = -\widetilde{M}_1^2 \mathcal{H}^\dagger \mathcal{H} + \widetilde{M}_2^2 \phi^* \phi + \widetilde{M}_3^2 (\phi^2 + \phi^{*2}) + \frac{C_3}{\sqrt{2}}(\phi + \phi^*). \quad (3.10)$$

The coupling constants which appear above are related to the parameters of the model Lagrangian as follows

$$\lambda_2 = \frac{\delta_{\lambda_2}}{2}(1 - \cos 2\beta) + \frac{\delta_{\mu_1} \mu}{F} \sin 2\beta + \frac{1}{F^2} [2\delta_{C_3} \delta_{\mu_1} (1 - \cos 2\beta) + \frac{\mu^2 m_A^2}{2}(1 + \cos^2 2\beta) + \frac{m_Z^4}{4} \cos^2 2\beta + (\widetilde{m}_s^2 + \widetilde{m}_p^2) \left( \frac{m_A^2}{4} \sin^2 2\beta - \mu^2 \right) + \frac{m_Z^2}{2} \cos^2 2\beta (3\mu^2 - \widetilde{m}_s^2 - \widetilde{m}_p^2)], \quad (3.11)$$

$$\lambda_3 = \delta_{\lambda_3} + \frac{1}{F^2} \left[ \frac{1}{4}(\widetilde{m}_s^2 + \widetilde{m}_p^2)^2 + \frac{1}{8}(\widetilde{m}_s^2 - \widetilde{m}_p^2)^2 + 4\delta_{\mu_2} \delta_{C_3} \right], \quad (3.12)$$

$$\lambda_4 = \frac{\delta_{\lambda_4}}{2}(1 - \cos 2\beta) + \frac{\delta_{\mu_1}\mu}{4F} \sin 2\beta + \frac{\delta_{C_3}\delta_{\mu_1}}{F^2}(1 - \cos 2\beta) + \frac{\widetilde{m}_s^2 - \widetilde{m}_p^2}{2F^2} \left[ \frac{m_A^2}{4} \sin^2 2\beta - \mu^2 - \frac{m_Z^2}{2} \cos^2 2\beta \right], \quad (3.13)$$

$$\lambda_5 = \delta_{\lambda_5} + \frac{1}{F^2} \left[ \frac{(\widetilde{m}_s^2 - \widetilde{m}_p^2)^2}{16} + 2\delta_{\mu_3}\delta_{C_3} \right], \quad (3.14)$$

$$\lambda_6 = \delta_{\lambda_6} + \frac{1}{F^2} \left[ \frac{\widetilde{m}_s^4 - \widetilde{m}_p^4}{4} + 2(\delta_{\mu_2} + \delta_{\mu_3})\delta_{C_3} \right], \quad (3.15)$$

$$\frac{\mu_1}{\sqrt{2}} = \frac{\delta_{\mu_1}}{2}(1 - \cos 2\beta) - \frac{\mu^3}{F} \sin 2\beta + \frac{\delta_{C_3}}{F^2} \left[ \frac{m_A^2}{2} \sin^2 2\beta - 2\mu^2 - m_Z^2 \cos^2 2\beta \right], \quad (3.16)$$

$$\frac{\mu_2}{\sqrt{2}} = \delta_{\mu_2} + \frac{\delta_{C_3}}{2F^2}(3\widetilde{m}_s^2 + \widetilde{m}_p^2), \quad (3.17)$$

$$\frac{\mu_3}{\sqrt{2}} = \delta_{\mu_3} + \frac{\delta_{C_3}}{2F^2}(\widetilde{m}_s^2 - \widetilde{m}_p^2), \quad (3.18)$$

$$\widetilde{M}_2^2 = \frac{\widetilde{m}_s^2 + \widetilde{m}_p^2}{2} + \frac{2\delta_{C_3}^2}{F^2}, \quad (3.19)$$

$$\widetilde{M}_3^2 = \frac{\widetilde{m}_s^2 - \widetilde{m}_p^2}{4} + \frac{\delta_{C_3}^2}{F^2}, \quad (3.20)$$

$$\frac{C_3}{\sqrt{2}} = \delta_{C_3}. \quad (3.21)$$

These expressions are obtained from (3.1) by substituting (3.6) and expanding in powers of  $1/F$ ; all the terms suppressed by  $1/F^3$  and stronger are neglected.

Next, we express the scalar fields as follows

$$\mathcal{H} = \frac{1}{\sqrt{2}} \begin{pmatrix} G^+ \\ h + iG^0 \end{pmatrix}, \quad \phi = \frac{1}{\sqrt{2}}(s + ip). \quad (3.22)$$

Here  $h$  is the Higgs field while real field  $G^0$  and complex field  $G^+$  are Goldstone bosons,  $s$  and  $p$  are scalar and pseudoscalar sgoldstinos. Substituting formulas (3.22) into (3.7)–(3.10) we obtain the tree-level zero-temperature potential  $V_0(h, s, p)$  of three scalar fields  $h, s, p$

$$V_0(h, s, p) = \frac{\lambda_1}{4}h^4 + \frac{\lambda_{hs}}{4}h^2s^2 + \frac{\lambda_{hp}}{4}h^2p^2 + \frac{\lambda_s}{4}s^4 + \frac{\lambda_p}{4}p^4 + \frac{\lambda_{sp}}{4}s^2p^2 + \frac{\mu_1}{2}sh^2 + \frac{\mu_s}{6}s^3 + \frac{\mu_{sp}}{2}sp^2 - \frac{\widetilde{M}_1^2}{2}h^2 + \frac{M_s^2}{2}s^2 + \frac{M_p^2}{2}p^2 + C_3s. \quad (3.23)$$

Here for convenience we introduce new coupling constants

$$\begin{aligned} \lambda_{hs} &\equiv \lambda_2 + 2\lambda_4, & \lambda_s &\equiv \lambda_3 + 2\lambda_5 + 2\lambda_6, & \lambda_p &\equiv \lambda_3 + 2\lambda_5 - 2\lambda_6, \\ \lambda_{hp} &\equiv \lambda_2 - 2\lambda_4, & \mu_s &\equiv 3(\mu_2 + \mu_3), & \mu_{sp} &\equiv \mu_2 - 3\mu_3, \\ \lambda_{sp} &\equiv 2\lambda_3 - 12\lambda_5, & M_s^2 &\equiv \widetilde{M}_2^2 + 2\widetilde{M}_3^2, & M_p^2 &\equiv \widetilde{M}_2^2 - 2\widetilde{M}_3^2. \end{aligned} \quad (3.24)$$



Let us note that in (3.23) the terms with Goldstone bosons have been omitted. We will take them into account later on in the calculation of field-dependent particle masses and the effective potential.

In the present scenario we assume that sgoldstino field does not acquire non-zero vacuum expectation value at zero temperature. In order to fix position of the minimum of tree level potential  $V_0(h, s, p)$  at the point  $\langle h \rangle = v$ ,  $\langle s \rangle = \langle p \rangle = 0$ , with  $v = 246$  GeV, in what follows we set parameters  $\widetilde{M}_1^2$  and  $C_3$  to be

$$\widetilde{M}_1^2 = \lambda_1 v^2, \quad C_3 = -\mu_1 v^2/2. \quad (3.25)$$

One-loop corrections to the potential  $V_0(h, s, p)$  at zero temperature in the form of Coleman-Weinberg potential in  $\overline{MS}$ -scheme [43] look as

$$V_{CW}(h, s, p) = \frac{1}{64\pi^2} \sum_i (-1)^{s_i} n_i m_i^4(h, s, p) \left( \log \frac{m_i^2(h, s, p)}{Q^2} - c_i \right), \quad (3.26)$$

where the sum goes over all fields of the model;  $Q$  is the renormalization scale and in our calculations we set  $Q = 100$  GeV. Contributions from bosons come with “+” sign, i.e.  $s_i = 0$ , fermion terms are summed with “-” sign,  $s_i = 1$ . In (3.26) the particle masses  $m_i(h, s, p)$  depend on background values of the scalar fields  $h, s, p$ . For each particle  $n_i$  is the number of its degrees of freedom,  $c_i = 3/2$  for scalar particles and fermions,  $c_i = 5/6$  for massive vector particles.

Field-dependent squared masses of the scalars  $h, s, p$  are the eigenvalues of the Hessian matrix of the potential (3.23),

$$\begin{pmatrix} V_{0,hh} & V_{0,hs} & V_{0,hp} \\ V_{0,hs} & V_{0,ss} & V_{0,sp} \\ V_{0,hp} & V_{0,sp} & V_{0,pp} \end{pmatrix}, \quad (3.27)$$

where

$$V_{0,hh} = 3\lambda_1 h^2 + \frac{\lambda_{hs}}{2} s^2 + \mu_1 s + \frac{\lambda_{hp}}{2} p^2 - \widetilde{M}_1^2, \quad (3.28)$$

$$V_{0,hs} = \lambda_{hs} h s + \mu_1 h, \quad (3.29)$$

$$V_{0,hp} = \lambda_{hp} h p, \quad (3.30)$$

$$V_{0,ss} = \frac{\lambda_{hs}}{2} h^2 + 3\lambda_s s^2 + \frac{\lambda_{sp}}{2} p^2 + \mu_s s + M_s^2, \quad (3.31)$$

$$V_{0,sp} = \lambda_{sp} s p + \mu_{sp} p, \quad (3.32)$$

$$V_{0,pp} = \frac{\lambda_{hp}}{2} h^2 + \frac{\lambda_{sp}}{2} s^2 + 3\lambda_p p^2 + \mu_{sp} s + M_p^2. \quad (3.33)$$

In particular, we obtain the following expressions for the Higgs boson, sgoldstino scalar and pseudoscalar squared masses at zero temperature near the electroweak vacuum  $(v, 0, 0)$ :

$$m_{h,s}^2{}_{phys} = \lambda_1 v^2 + \frac{\lambda_{hs}}{4} v^2 + \frac{M_s^2}{2} \pm \sqrt{\left( \lambda_1 v^2 - \frac{\lambda_{hs}}{4} v^2 - \frac{M_s^2}{2} \right)^2 + \mu_1^2 v^2}, \quad (3.34)$$

$$m_p^2{}_{phys} = \frac{\lambda_{hp}}{2}v^2 + M_p^2. \quad (3.35)$$

The tree-level squared field-dependent masses of top-quark,  $Z$ ,  $W^\pm$ -bosons are as usual

$$m_t^2(h) = \frac{y_t^2}{2}h^2, \quad m_Z^2(h) = \frac{g'^2 + g^2}{4}h^2, \quad m_W^2(h) = \frac{g^2}{4}h^2, \quad (3.36)$$

here  $y_t$  is the Yukawa coupling constant of top-quark,  $g'$  and  $g$  are the  $U(1)_Y$  and  $SU(2)_W$  coupling constants, while squared mass of Goldstone bosons  $G^0$ ,  $G^\pm$  is

$$m_G^2(h, s, p) = \lambda_1 h^2 + \frac{\lambda_{hs}}{2}s^2 + \mu_1 s + \frac{\lambda_{hp}}{2}p^2 - \widetilde{M}_1^2. \quad (3.37)$$

In general, quantum corrections to the effective potential represented by  $V_{CW}(h, s, p)$  shift the position of the tree level potential minimum. In order to fix the minimum at zero temperature at the point  $(v, 0, 0)$  as well as to fix values of scalar particle masses in this minimum, we add the following counterterms

$$V_{CT}(h, s, p) = \frac{\delta\lambda_1}{4}h^4 + \frac{\delta\lambda_{hs}}{4}h^2s^2 + \frac{\delta\lambda_{hp}}{4}h^2p^2 + \frac{\delta\mu_1}{2}sh^2 - \frac{\delta\widetilde{M}_1^2}{2}h^2 + \delta C_3 s. \quad (3.38)$$

Coefficients  $\delta\lambda_1, \delta\lambda_{hs}, \delta\lambda_{hp}, \delta\mu_1, \delta\widetilde{M}_1^2, \delta C_3$  in the counterterm potential  $V_{ct}(h, s, p)$  are chosen in such a way that all the first and the second partial derivatives of the sum  $V_{CW} + V_{ct}$  with respect to fields  $h, s, p$  are equal to zero at the point  $(v, 0, 0)$  [44], which results in

$$\delta\lambda_1 = -\frac{1}{2v^2} \left. \frac{\partial^2 V_{CW}}{\partial h^2} \right|_{(v,0,0)} + \frac{1}{2v^3} \left. \frac{\partial V_{CW}}{\partial h} \right|_{(v,0,0)}, \quad (3.39)$$

$$\delta\lambda_{hs} = -\frac{2}{v^2} \left. \frac{\partial^2 V_{CW}}{\partial s^2} \right|_{(v,0,0)}, \quad \delta\lambda_{hp} = -\frac{2}{v^2} \left. \frac{\partial^2 V_{CW}}{\partial p^2} \right|_{(v,0,0)}, \quad (3.40)$$

$$\delta\mu_1 = -\frac{1}{v} \left. \frac{\partial^2 V_{CW}}{\partial h \partial s} \right|_{(v,0,0)}, \quad \delta C_3 = -\left. \frac{\partial V_{CW}}{\partial s} \right|_{(v,0,0)} + \frac{v}{2} \left. \frac{\partial^2 V_{CW}}{\partial h \partial s} \right|_{(v,0,0)}, \quad (3.41)$$

$$\delta\widetilde{M}_1^2 = -\frac{1}{2} \left. \frac{\partial^2 V_{CW}}{\partial h^2} \right|_{(v,0,0)} + \frac{3}{2v} \left. \frac{\partial V_{CW}}{\partial h} \right|_{(v,0,0)}. \quad (3.42)$$

Full expression for the scalar potential of the model at zero temperature reads

$$V_{T=0}(h, s, p) = V_0(h, s, p) + V_{CW}(h, s, p) + V_{CT}(h, s, p). \quad (3.43)$$

To summarize, with all the assumptions described above the model scalar potential (3.23) is fully specified by the following parameters

$$\lambda_s, \lambda_p, \lambda_{hs}, \lambda_{hp}, \lambda_{sp}, \lambda_{hp}, \mu_1, \mu_s, \mu_{sp}, \quad (3.44)$$

as well as masses  $m_{s phys}, m_{p phys}$  and  $m_{h phys} = 125$  GeV. As an input for the analysis of the EWPT dynamics we use these parameters taken directly at the electroweak

scale, i.e. at  $Q \sim 100$  GeV, while other quantities entering (3.23) can be found from (3.25) which fixes the position of the minimum at zero temperature and the expressions (3.34) and (3.35). In due course we will discuss relation to the parameters of supersymmetric model.

The one-loop effective potential at finite temperature includes the following thermal corrections (the free energy density of plasma) [45]

$$V_T(T, h, s, p) = \frac{T^4}{2\pi^2} \sum_i n_i J_{B/F} \left( \frac{m_i(h, s, p)}{T} \right), \quad (3.45)$$

where  $T$  is temperature, and the sum is taken over all particle species that are in thermal equilibrium in plasma. Special thermal functions  $J_B(x)$  for bosons and  $J_F(x)$  for fermions are defined as

$$J_{B/F}(x) = \pm \int_0^\infty dy y^2 \ln \left( 1 \mp \exp \left( -\sqrt{x^2 + y^2} \right) \right). \quad (3.46)$$

The integral (3.46) cannot be expressed in terms of analytical functions, although it can be expanded into series of MacDonald functions

$$J_{B/F}(x) = \mp x^2 \sum_{n=1}^{\infty} \frac{(\pm 1)^n}{n^2} K_2(nx). \quad (3.47)$$

It is known that validity of the perturbation theory for the effective potential breaks down at high temperatures. This problem can be cured by resummation of daisy diagrams (see, e.g. [46, 47]) which yields the following additional contribution to the effective potential

$$V_d(T, h, s, p) = -\frac{T}{12\pi} \sum_i a_i n_i \left( (m_{T_i}^2(T, h, s, p))^{3/2} - (m_i^2(h, s, p))^{3/2} \right), \quad (3.48)$$

where  $a_i = 1$  for scalars and  $a_i = 1/3$  for vector bosons. While ordinary particle masses  $m_i^2$  are eigenvalues of the mass matrix  $\mathcal{M}^2$ , the thermal Debye masses  $m_{T_i}^2$  are the eigenvalues of the full mass matrix  $\mathcal{M}^2 + \Pi(T)$  that includes thermal corrections. For the Higgs boson  $h$  and sgoldstinos  $s, p$  the thermal corrections to the squared mass matrix have the form  $\Pi(T) = \text{diag}(\Pi_h, \Pi_s, \Pi_p)$ , where

$$\Pi_h(T) = T^2 \left( \frac{\lambda_1}{2} + \frac{\lambda_{hs} + \lambda_{hp}}{24} + \frac{3g^2 + g'^2}{16} + \frac{y_t^2}{4} \right), \quad (3.49)$$

$$\Pi_s(T) = T^2 \left( \frac{\lambda_{hs}}{6} + \frac{\lambda_s}{4} + \lambda_{sp} \right), \quad (3.50)$$

$$\Pi_p(T) = T^2 \left( \frac{\lambda_{hp}}{6} + \frac{\lambda_p}{4} + \lambda_{sp} \right). \quad (3.51)$$

Debye corrections for the Goldstone bosons are

$$\Pi_{G^0, G^\pm}(T) = T^2 \left( \frac{\lambda_1}{2} + \frac{\lambda_{hs} + \lambda_{hp}}{24} + \frac{3g^2 + g'^2}{16} + \frac{y_t^2}{4} \right). \quad (3.52)$$

Masses of transverse components of the vector bosons do not acquire Debye corrections, while the mass squared of longitudinal component of  $W$ -boson receive thermal correction  $\Pi_{W_L}(T) = \frac{11}{6}g^2T^2$ . The full mass matrix of photon and  $Z$ -boson longitudinal components is

$$\mathcal{M}_{\gamma Z_L}^2 + \Pi_{\gamma Z_L}(T) = \begin{pmatrix} \frac{1}{4}g^2h^2 + \frac{11}{6}g^2T^2 & \frac{1}{4}gg'h^2 \\ \frac{1}{4}gg'h^2 & \frac{1}{4}g'^2h^2 + \frac{11}{6}g'^2T^2 \end{pmatrix} \quad (3.53)$$

Sum of (3.43), (3.45) and (3.48) gives the one-loop finite-temperature effective potential of the model

$$V_{\text{eff}}(T, h, s, p) = V_{T=0}(h, s, p) + V_T(T, h, s, p) + V_d(T, h, s, p). \quad (3.54)$$

Let us comment briefly on known theoretical uncertainties inherent in utilizing the effective potential in the form (3.54). Firstly, it is known that the effective potential is explicitly gauge dependent [48, 49] and we use the effective potential calculated in the Landau gauge. Secondly, we truncate the perturbative expansion, keeping only the one-loop order terms, which imposes the dependence on the renormalization scale. The two-loop analysis of EWPT in a singlet-extended SM performed recently [50] has revealed that the two-loop corrections may change the values of the critical temperature and the latent heat by 20–50% (up to 100%) depending on the model. In respect to these issues, we refer to the recent review [51] for an extensive discussion of various theoretical uncertainties typical in investigations of the cosmological first order phase transitions. One should bear in mind those uncertainties when applying the numerical results presented in the rest of the paper.

## 4 Numerical results

In this Section we investigate the possibility of getting the first order electroweak phase transition in the supersymmetric model with relatively light sgoldstinos and calculate the spectrum of gravitational waves produced during this transition. Since the model parameter space is multidimensional and large, we do not perform scanning over it to indicate the regions where the EWPT is of the first order, but rather present several points in this space, where we checked the EWPT is of the first order and studied the generation of gravitational waves.

As to the found benchmark points, we recall that generically the first order EWPT occurs in very specific parts of the model parameter space and even small shifts of the parameters can change properties of the phase transition drastically.

Nevertheless, the chosen points are in a rather compact region of the model parameter space. And as we found the first order EWPT in each of them (though with different characteristics) we certainly can claim that this phenomenon is not unique for these sets of parameters. At the same time we calculate the spectra of gravitational waves produced during the EWPT in each case and found that even within this compact part of the parameter space the model predicts wide range of peak frequency and amplitude of this spectrum. Finally, we illustrated the impact of some theoretical uncertainties discussed in the previous Section on the model predictions.

#### 4.1 First-order electroweak phase transition

The dynamics of EWPT is determined by the effective potential (3.54). The numerical package `PhaseTracer` [52] was used to search for the models in the parameter space for which the first-order electroweak phase transition takes place and explore its properties. Besides, the thermal functions (3.46) were computed using the numerical library `thermal_funcs` [53]. With the help of this software we can obtain the value of potential (3.54) and its minima positions in the field space as functions of temperature  $T$ . We select several benchmark models dubbed  $Q_1, \dots, Q_{10}$  in which (as we have found) the first order phase transition takes place. In Table 1 we present

BM	$\lambda_{hs}$	$\lambda_{hp}$	$\lambda_s$	$\lambda_p$	$\lambda_{sp}$	$T_{\text{nuc}}$	$T_{\text{perc}}$	$\alpha \cdot 10^3$	$\beta/H_c$	$g_*$
$Q_1$	0.88	0.78	0.70	0.60	0.70	63.58	58.30	119	254	107.25
$Q_2$	0.85	0.75	0.70	0.60	0.70	81.51	78.22	37.4	602	107.75
$Q_3$	0.80	0.70	0.70	0.60	0.70	99.60	97.64	15.2	1470	107.75
$Q_4$	0.75	0.65	0.70	0.60	0.70	112.25	111.05	8.61	2920	107.75
$Q_5$	0.70	0.65	0.70	0.60	0.70	122.06	121.36	5.48	5760	107.75
$Q_6$	0.65	0.60	0.70	0.60	0.70	130.07	129.72	3.52	12700	107.75
$Q_7$	0.60	0.50	0.55	0.45	0.60	133.45	133.13	2.88	15700	107.75
$Q_8$	0.60	0.50	0.60	0.50	0.70	134.84	134.61	2.56	19400	107.75
$Q_9$	0.60	0.50	0.65	0.55	0.70	135.85	135.66	2.26	27800	107.75
$Q_{10}$	0.60	0.40	0.70	0.60	0.70	136.74	136.61	1.95	38100	107.75

**Table 1:** Dimensionless parameters of selected benchmark models (BM) with the first order electroweak phase transition as well as nucleation and percolation temperatures  $T_{\text{nuc}}, T_{\text{perc}}$  (in GeV), strength  $\alpha$ , ratio  $\beta/H_c$  and effective number of degrees of freedom  $g_*$ .

the values, which dimensionless parameters  $\lambda_{hs}, \lambda_{hp}, \lambda_s, \lambda_p$  and  $\lambda_{sp}$  take in these models. As for other parameters, we fix  $\mu_1 = 5 \text{ GeV}$ ,  $\mu_s = 30 \text{ GeV}$ ,  $\mu_{sp} = -10 \text{ GeV}$  and choose  $m_s \text{ phys} = 110 \text{ GeV}$ ,  $m_p \text{ phys} = 440 \text{ GeV}$  for concreteness.

Let us note that the first order phase transition in a SM extension with scalar singlet typically requires large coupling between the Higgs boson and the scalar, see

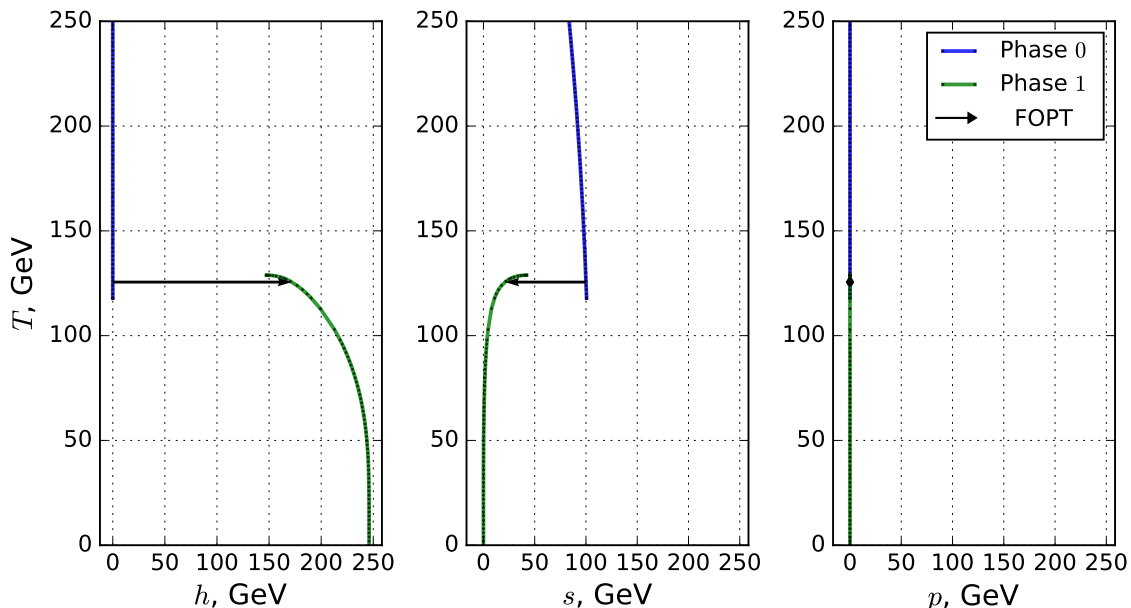


**Figure 1:** Temperature dependence of field values at the minimum of the effective potential for the benchmark model  $Q_5$ , see Table 1. The full list of parameter values is given in the text. This graph is plotted using the package `PhaseTracer` [52].

e.g. [30, 32, 44, 54]. Indeed, the deformation of the Higgs effective potential, needed to replace the expected in the SM crossover with the first order EWPT, naturally implies a sufficiently strong Higgs interaction with the new scalar(s). Then the models with light enough sgoldstinos would admit the Higgs boson decays  $h \rightarrow ss$  or  $h \rightarrow pp$  with unacceptably large partial widths. On the other hand, the scalar potential with heavy sgoldstinos would not lead to the first order EWPT, because their contribution to the thermal dynamics will be suppressed by the mass, and the form of the Higgs effective potential remains similar to that in the SM. Figure 1 shows an example of minimum positions depending on temperature for the benchmark point  $Q_5$  with model parameters shown in Table 1. In this example the value of pseudoscalar sgoldstino field  $\langle p \rangle = 0$  at any temperature. At high temperatures there exists only a single phase with  $\langle h \rangle = 0$  and  $\langle s \rangle \neq 0$ . At  $T = 129$  GeV another phase with broken electroweak symmetry, i.e. when  $\langle h \rangle \neq 0$  and  $\langle s \rangle = 0$ , naturally appears. The arrow in Figure 1 marks the critical temperature  $T_c = 126$  GeV at which these two phases have equal values of the effective potential. The electroweak phase transition for other benchmark models in Table 1 exhibit the similar dynamics. Let us note that despite  $\langle p \rangle = 0$  at any temperature, the effective potential still depends on the dimensionless parameters  $\lambda_{hp}$ ,  $\lambda_p$ ,  $\lambda_{sp}$  as they contribute to thermal corrections (3.49)–(3.51).

The phase transition starts when bubbles of new phase begin to nucleate in the

Universe. The bubble production rate per unit volume is given by [55, 56]

$$P \sim \mathcal{A}(T) \exp\left\{-\frac{S_3}{T}\right\}, \quad (4.1)$$

where  $\mathcal{A}(T)$  is a dynamical prefactor and  $S_3$  is  $O(3)$ -symmetric Euclidean action

$$S_3 = \int_0^\infty 4\pi\rho^2 d\rho \left( V_{\text{eff}}(T, h, s, p) + \frac{1}{2} \left(\frac{dh}{d\rho}\right)^2 + \frac{1}{2} \left(\frac{ds}{d\rho}\right)^2 + \frac{1}{2} \left(\frac{dp}{d\rho}\right)^2 \right), \quad (4.2)$$

calculated on the bounce solution, with  $\rho$  being radial coordinate. The bounce is a spherically symmetric solution of the classical field equations [57]

$$\frac{d^2\varphi_i}{d\rho^2} + \frac{2}{\rho} \frac{d\varphi_i}{d\rho} = \frac{\partial V_{\text{eff}}}{\partial\varphi_i}, \quad (4.3)$$

where  $\varphi_i$  stands for  $h$ ,  $s$  or  $p$ . The equation (4.3) is supplemented with the following boundary conditions: 1)  $\frac{d\varphi_i(\rho)}{d\rho} = 0$  at  $\rho = 0$ ; 2)  $\varphi_i(\rho) \rightarrow \varphi_i^{\text{false}}$  at  $\rho \rightarrow \infty$ , where  $\varphi_i^{\text{false}}$  are values of the fields in the false minimum. The nucleation in the primordial plasma starts at temperature  $T_{\text{nuc}}$ , when the factor in exponent (4.1) drops to  $\frac{S_3}{T}|_{T=T_{\text{nuc}}} \simeq 140$  [58].

To find numerically the bounce solution and calculate the action  $S_3$  entering (4.1) we use the package `FindBounce` [59]. Figure 2 shows an example of bounce profile in space at temperature  $T \approx 122$  GeV. To find the nucleation temperature  $T_{\text{nuc}}$  we solve numerically equation  $\frac{S_3}{T}|_{T=T_{\text{nuc}}} = 140$ .

After the temperature reaches  $T_{\text{nuc}}$ , more and more bubbles nucleate and the latent heat of the unbroken phase releases. The bubbles of new phase expand decreasing the fraction of the Universe in the metastable state. The phase transition is completed after the bubble percolation which happens at the temperature  $T_{\text{perc}}$  to be found [60] from the equation

$$\frac{S_3(T_{\text{perc}})}{T_{\text{perc}}} = 131 + \log\left(\frac{A}{T^4}\right) - 4 \log\left(\frac{T}{100 \text{ GeV}}\right) - 4 \log\left(\frac{\beta(T_{\text{perc}})/H_c}{100}\right) + 3 \log v_w, \quad (4.4)$$

where  $\log\left(\frac{A}{T^4}\right) \approx -14$  for EWPT [61] and  $v_w$  is the bubble wall velocity. In this study we take  $v_w = 0.55$  as an exemplary value assuming deflagration for the bubble growth regime (see e.g. [62–65] for discussion of velocity calculation).

There are several other important parameters which determine the gravitational wave signal from the first order phase transitions, see e.g. [60, 66]. Parameter  $\alpha$  characterizes the strength of the phase transition. It is the ratio of the latent heat density (heat released during the phase transition) to the radiation energy density

$$\alpha \equiv \left(\frac{g_*\pi^2 T_{\text{perc}}^4}{30}\right)^{-1} \left(\Delta V_{\text{eff}} - \frac{T}{4} \frac{d\Delta V_{\text{eff}}}{dT}\right) \Big|_{T_{\text{perc}}}, \quad (4.5)$$

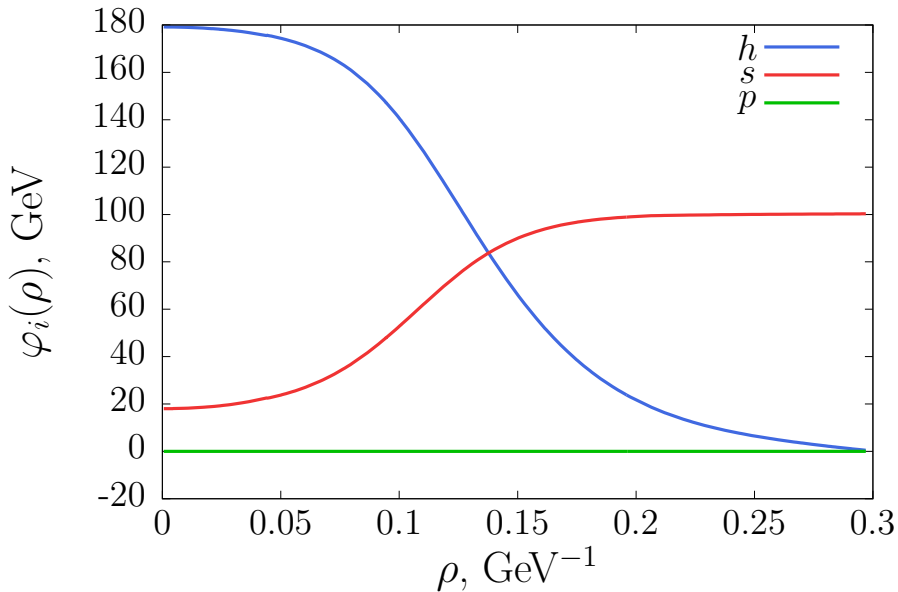


**Figure 2:** Profile of the bounce solution for the benchmark model  $Q_5$  at the nucleation temperature. Blue (top), red (middle) and green (bottom) curves correspond to  $h$ ,  $s$  and  $p$ , respectively. The field  $\varphi_i$  value in GeV is on the vertical axis, the distance to the origin in 3-dimensional space  $\rho$  in  $\text{GeV}^{-1}$  is on the horizontal axis. The origin is in the bubble center. This graph was plotted using the package `FindBounce` [59].

where  $g_*$  is the total effective number of degrees of freedom which are in thermal equilibrium in plasma,  $\Delta V_{\text{eff}}$  is the potential value difference between the broken and unbroken phases. Another parameter  $\beta/H_c$  characterises the (inverse) timescale of the phase transition and reads

$$\frac{\beta}{H_c} \equiv T \left. \frac{d}{dT} \left( \frac{S_3}{T} \right) \right|_{T_{\text{perc}}} . \quad (4.6)$$

We calculate  $\alpha$  and  $\beta/H_c$  for the selected set of benchmark models and present them in Table 1 along with nucleation and percolation temperatures,  $T_{\text{nuc}}$  and  $T_{\text{perc}}$  as well as effective number of degrees of freedom  $g_*$ .

## 4.2 Gravitational waves

Calculation of spectrum of gravitational waves produced during a first-order phase transition was a subject of numerous recent studies. Here we follow [60, 66] to estimate the GW power spectrum produced during the EWPT within the model with light sgoldstinos. For phase transitions found in this work the gravitational wave signal is mostly produced by sound waves and magnetohydrodynamic (MHD) turbulence in plasma, while the impact of released kinetic energy of bubble walls can



be neglected. The relative contribution of gravitational waves to the present energy density of the Universe reads

$$\Omega_{\text{GW}}h^2 = \Omega_{\text{sw}}h^2 + \Omega_m h^2, \quad (4.7)$$

where the first term comes from sound waves and the second one is the MHD turbulence contribution;  $h \simeq 0.7$  is the value of the Hubble constant in terms of 100 (km/s)/Mpc. The general form of such signal spectra are usually parametrized as

$$\Omega_{\text{sw}}h^2 = 1.23 \cdot 10^{-5} \frac{v_w H_c}{g_*^{1/3} \beta} \left( \frac{\kappa_{\text{sw}} \alpha}{1 + \alpha} \right)^2 S_{\text{sw}}(f) \Upsilon, \quad (4.8)$$

$$\Omega_m h^2 = 1.55 \cdot 10^{-3} \frac{v_w H_c}{g_*^{1/3} \beta} \left( \frac{\kappa_m \alpha}{1 + \alpha} \right)^{3/2} S_m(f), \quad (4.9)$$

where the bubble wall velocity  $v_w$  we fix to be equal 0.55 (a typical value for phase transitions),

$$\kappa_{\text{sw}} = \frac{c_s^{11/5} k_a k_b}{\left( c_s^{11/5} - v_w^{11/5} \right) k_b + v_w c_s^{6/5} k_a}, \quad \kappa_m = 0.05 \kappa_{\text{sw}}, \quad c_s = \frac{1}{\sqrt{3}}, \quad (4.10)$$

$$k_a = \frac{6.9 v_w^{6/5} \alpha}{1.36 - 0.037 \sqrt{\alpha} + \alpha}, \quad k_b = \frac{\alpha^{2/5}}{0.017 + (0.9997 + \alpha)^{2/5}}, \quad (4.11)$$

$S_{\text{sw}}(f)$  and  $S_m(f)$  are the spectrum shapes,

$$S_{\text{sw}}(f) = \left( \frac{f}{f_{\text{sw}}} \right)^3 \left( \frac{7}{4 + 3(f/f_{\text{sw}})^2} \right)^{7/2}, \quad (4.12)$$

$$S_m(f) = \frac{(f/f_m)^3}{(1 + f/f_m)^{11/3} \left( 1 + \frac{8\pi f}{h_*} \right)}, \quad (4.13)$$

where

$$h_* = 1.65 \cdot 10^{-5} \text{ Hz} \left( \frac{T}{100 \text{ GeV}} \right) \left( \frac{g_*}{100} \right)^{1/6} \quad (4.14)$$

and peak frequencies are given by

$$f_{\text{sw}} \simeq \frac{1.15 \beta h_*}{v_w H_c}, \quad f_m \simeq \frac{1.65 \beta h_*}{v_w H_c}. \quad (4.15)$$

The factor

$$\Upsilon = 1 - \frac{1}{\sqrt{1 + 2\tau_{\text{sw}} H_c}}, \quad (4.16)$$

where

$$\tau_{\text{sw}} H_c \sim (8\pi)^{1/3} \frac{v_w}{\beta/H_c} \bar{U}_f, \quad \bar{U}_f \sim \sqrt{\frac{3\alpha}{4(1+\alpha)} \kappa_{\text{sw}}} \quad (4.17)$$

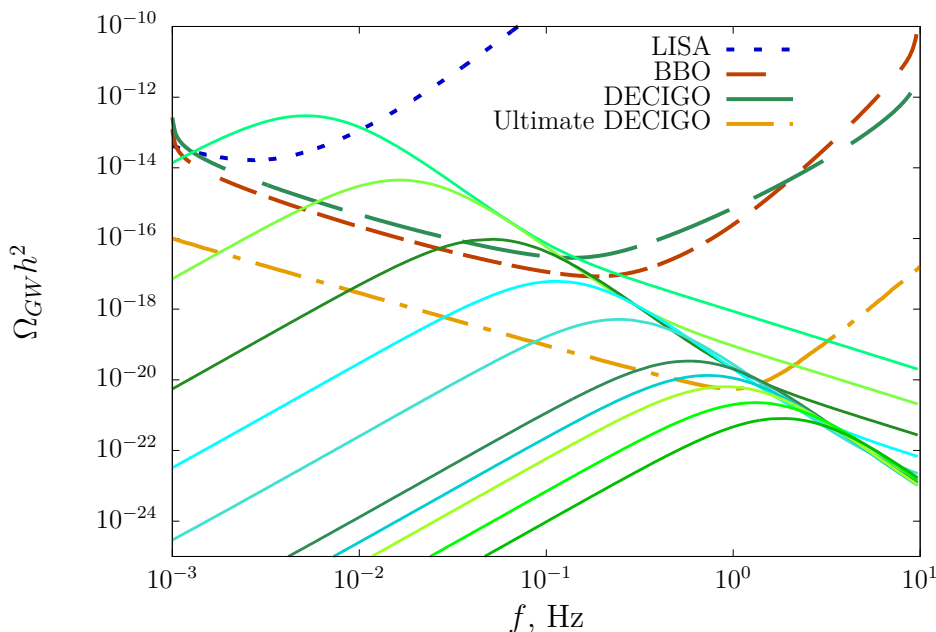


**Figure 3:** Gravitational wave spectra from the first-order phase transition for points  $Q_1, Q_2, \dots, Q_{10}$  (from top to bottom, solid lines) in model parameter space, see Table 1, and sensitivity curves of LISA, BBO, DECIGO, Ultimate DECIGO experiments (dashed lines) [41, 69].

accounts for the effective lifetime of acoustic wave as a source of gravitational waves, see refs. [67, 68].

The gravitational wave spectra obtained for points  $Q_1$ – $Q_{10}$  using data from Table 1 and (4.7)–(4.15) are shown in Figure 3. Maxima of these signals fall into the frequency range  $10^{-3}$ –10 Hz. Figure 3 also shows the sensitivity curves of the space gravitational wave observatories LISA, BBO, DECIGO and Ultimate DECIGO. One can see that these experiments can potentially register the predicted signals. The results shown in Figure 3 were obtained with renormalization scale  $Q = 100$  GeV. To partly estimate possible theoretical uncertainties in these predictions we study the dependence of the gravitational wave signal on our choice of the renormalization scale by varying it between  $Q/2$  and  $2Q$ . In Figure 4 we show predictions for GW power spectra for models  $Q_1$  and  $Q_5$  obtained with different values of the renormalization scale  $Q$ . For benchmark model  $Q_5$  the predicted signal varies within up to two orders of magnitude when calculated for  $Q$  from 50 to 200 GeV. At the same time for  $Q_1$  the similar difference for  $Q = 50$  and 100 GeV is much larger (of order  $10^3$ ) while for  $Q = 200$  GeV the electroweak phase transition is found not to take place. We also link the renormalization scale to the percolation temperature and plot our results for points  $Q_1, Q_3, Q_5$  as bands filled between the lines  $Q = T_{perc}/2$  and  $Q = 2T_{perc}$  with

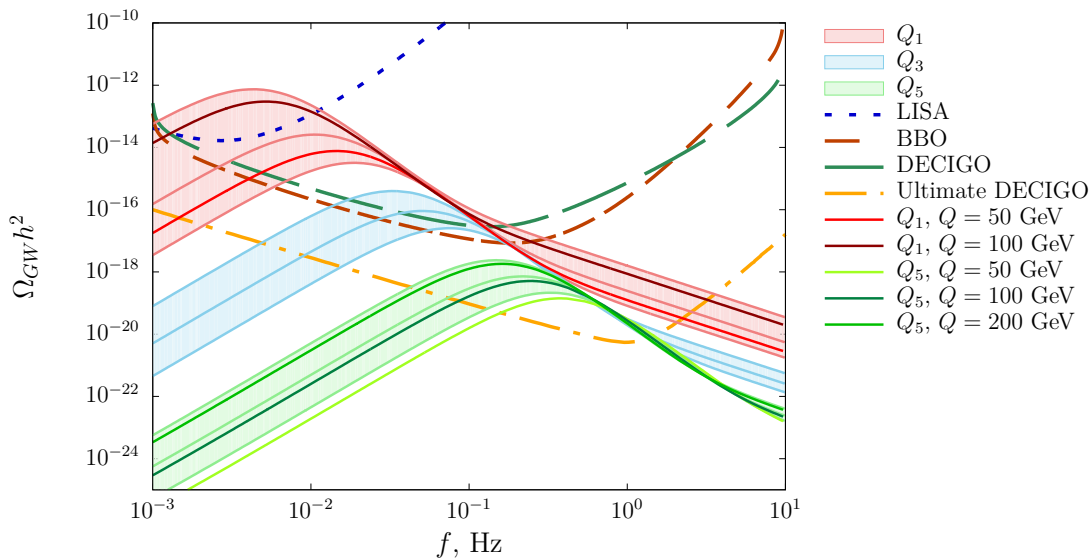


**Figure 4:** Solid lines: the gravitational wave spectra from the first-order phase transition for points  $Q_1$  and  $Q_5$  computed adopting the renormalization scale as  $Q = 50$  GeV,  $100$  GeV and  $200$  GeV. For point  $Q_1$  with  $Q = 200$  GeV the bubble nucleation does not take place. Filled bands: the GW spectra for points  $Q_1$ ,  $Q_3$ ,  $Q_5$  for the variation of the renormalization scale from  $2T_{perc}$  (upper edges) to  $T_{perc}/2$  (bottom edges) through  $T_{perc}$  (central lines).

the central line at  $Q = T_{perc}$ . This underlines considerable theoretical uncertainties pertinent to these predictions (see e.g. [70] for a recent discussion on this subject). Table 2 shows the changes in the phase transition parameters crucial for the GW spectra.

### 4.3 Relation to parameters of supersymmetric model

So far we conveniently discussed physics of the electroweak phase transition in terms of parameters entering the low-energy effective potential (3.23). Let us relate the parameters of the benchmark models shown in Table 1 to the coupling constants of the underlying supersymmetric model (2.1). As we use bottom-up approach and the corresponding higher energy theory has a lot of additional degrees of freedom, in deducing a viable scenario we have a selection of several mass scales, such as supersymmetry breaking scale  $\sqrt{F}$  and common scale of superpartners. The latter should be lower than  $\sqrt{F}$  as we discuss in Section 2. The dimensionless coupling constants of the chosen benchmark models turn out to be fairly large. Therefore, the possibility of perturbative treatment of the model up to the supersymmetry breaking scale requires absence of any Landau pole for these coupling constants up to  $\sqrt{F}$ . We exploit

BM	$Q$ , GeV	$T_{\text{nuc}}$ , GeV	$T_{\text{perc}}$ , GeV	$\alpha \cdot 10^3$	$\beta/H_c$	$g_*$
$Q_1$	109.7	60.71	54.88	168	228	97.25
	68.4	72.59	68.49	62.5	442	107.75
	39.3	81.75	78.63	35.9	683	107.75
$Q_3$	181.4	93.17	90.71	20.8	1040	107.75
	97.9	99.80	97.86	15.0	1490	107.75
	51.9	105.28	103.74	11.6	2060	107.75
$Q_5$	231.9	116.94	115.93	7.06	3670	107.75
	120.3	121.02	120.27	5.77	5190	107.75
	62.0	124.53	123.98	4.80	7530	107.75

**Table 2:** The renormalization scale  $Q$ , nucleation and percolation temperatures, parameters  $\alpha$  and  $\beta/H_c$  for BM  $Q_1$ ,  $Q_3$ ,  $Q_5$ . For each point we calculate the first order electroweak phase transition parameters taking the renormalization scale  $2T_{\text{perc}}$ ,  $T_{\text{perc}}$  and  $T_{\text{perc}}/2$ .

the renormalization group equations<sup>1</sup> to tie the parameters at the electroweak scale used in the study of EWPT to the parameters of the high energy theory imposing tree level matching conditions (3.11)–(3.21) for an illustration. Thus, in Table 3 we show three exemplary scenarios corresponding to the low-energy benchmark model  $Q_2$ . Namely, each column correspond to a particular choice of  $\sqrt{F}$ ,  $m_A$  and  $\mu$ .

The direct experimental constraints on  $\sqrt{F}$  are derived from collider searches for processes with missing energy signature and these constraints are of order a few TeV, see e.g. [71–74]. Direct searches for superpartners at ATLAS and CMS experiments [75–81] put model-dependent constraints on soft masses, in particular, on gluino mass. The lower bound on gluino mass in these experiments is lower than 3 TeV. In particular, interpretation of the LHC negative results for gluinos and squarks within GMSB-like scenarios put lower bounds on maximal values of soft SUSY breaking parameters of order 2 TeV, see e.g. [82]. Therefore, we choose values of  $\sqrt{F}$ ,  $m_A$  and  $\mu$  somewhat above this energy scale. Table 3 shows values of parameters of the low-energy theory at a scale  $Q$  about the superpartner masses. We have checked for each of the benchmark model that position of the Landau pole (if any) for each coupling is well above the supersymmetry breaking scale, see appendix. It justifies the description of the EWPT entirely in terms of the effective field theory we adopted. As it can be valid up to the energy scale much higher than the electroweak scale, the model phenomenology at LHC can be also described in terms of the effective scalar potential and two new ingredients – sgoldstinos. From Tables 1 and 3 we see that dimensionless coupling constants in the scalar sector, in particular, those responsible for interaction between sgoldstino and Higgs fields, are of order unity. This is a

<sup>1</sup>We present the set of RGE equations for the low energy model in appendix.

$\sqrt{F}$ , TeV	10	30	100
$m_A$ , TeV	3.5	7.0	9.0
$\mu$ , TeV	-2.5	-6.0	-8.0
$Q$ , TeV	4	8	10
$\lambda_1(Q)$	0.0978	0.0962	0.0961
$\lambda_2(Q)$	1.10	1.18	1.20
$\lambda_3(Q)$	0.866	0.952	0.984
$\lambda_4(Q)$	0.0421	0.0472	0.0491
$\lambda_5(Q)$	0.0565	0.0624	0.0645
$\lambda_6(Q)$	0.0536	0.0641	0.0681
$\mu_1(Q)$ , GeV	6.78	7.23	7.39
$\mu_2(Q)$ , GeV	8.54	9.65	10.1
$\mu_3(Q)$ , GeV	6.40	6.81	6.96
$\tilde{M}_1^2(Q)$ , GeV <sup>2</sup>	$5.15 \cdot 10^3$	$4.39 \cdot 10^3$	$4.13 \cdot 10^3$
$\tilde{M}_2^2(Q)$ , GeV <sup>2</sup>	$88.5 \cdot 10^3$	$91.0 \cdot 10^3$	$91.9 \cdot 10^3$
$\tilde{M}_3^2(Q)$ , GeV <sup>2</sup>	$-50.1 \cdot 10^3$	$-51.0 \cdot 10^3$	$-51.4 \cdot 10^3$
$C_3(Q)$ , GeV <sup>3</sup>	$-210 \cdot 10^3$	$-222 \cdot 10^3$	$-226 \cdot 10^3$
$\delta_{\lambda_2}$	1.11	1.19	1.21
$\delta_{\lambda_3}$	0.866	0.952	0.984
$\delta_{\lambda_4}$	0.0424	0.0476	0.0496
$\delta_{\lambda_5}$	0.0565	0.0624	0.0645
$\delta_{\lambda_6}$	0.0536	0.0641	0.0681
$\delta_{\mu_1}$ , GeV	-26.4	-42.8	-4.97
$\delta_{\mu_2}$ , GeV	6.04	6.83	7.12
$\delta_{\mu_3}$ , GeV	4.53	4.82	4.92
$\delta_{C_3}$ , GeV <sup>3</sup>	$-149 \cdot 10^3$	$-157 \cdot 10^3$	$-160 \cdot 10^3$

**Table 3:** Reconstruction of physical parameters at high energies for the benchmark model  $Q_2$  with  $\tan\beta = 10$ .

generic feature for all our benchmark points, indicating that existence of the first order EWPT requires interactions of additional scalar degrees of freedom with the Higgs boson not to be weak [83]. Looking at the matching conditions (3.11)–(3.21) one concludes that for chosen values of model parameters and given the hierarchies  $m_{soft}, \mu \lesssim \sqrt{F}$  and  $m_{s,phys}, m_{p,phys} \ll \sqrt{F}$  it is difficult (if not impossible) to obtain such large values of  $\lambda_2$  and  $\lambda_3$  without introducing the ‘ $\delta$ ’-set of operators in the Kähler potential in (2.5). The viable choices of values of the corresponding coupling constants behind these operators are presented in Table 3 for completeness. Here we set  $\tan\beta = 10$ .

Finally, let us briefly discuss possible collider phenomenology of presented sce-

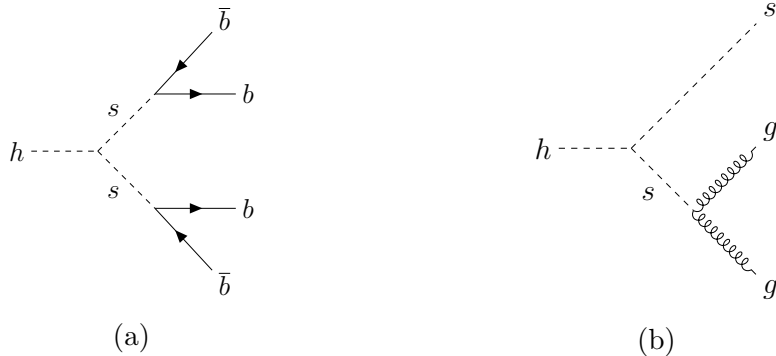


**Figure 5:** Possible exotic Higgs boson decays with sgoldstino involved.

nario associated with that part of the model, which is responsible for the first order electroweak phase transition. The new lightest degree of freedom, scalar sgoldstino, can show up in several signatures. The details are defined in particular by the scalar potential (3.23) describing sgoldstino interactions with the Higgs boson. As for interactions of sgoldstino with other SM particles they are fixed by terms in the Lagrangian (2.2), (2.3), (2.4) whose couplings are determined by the soft parameters. The sgoldstino direct production is naturally dominated by the gluon fusion. Its rate crucially depends on the relation between soft gluino mass  $M_3$  and supersymmetry breaking scale and thus is largely model dependent. Prospects of such searches and bounds from existing experimental results have been discussed in several studies previously, see e.g. [18, 24, 74, 84]. In general, sgoldstino can reveal themselves either through mixing with the Higgs boson or via triple and quartic interactions involving the Higgs boson and sgoldstino. The sgoldstino-Higgs mixing angle is determined by the mass matrix (3.27) and for the found benchmark models it can be quite prominent. In particular, the sine squared of the mixing angle between scalar sgoldstino and the Higgs boson can reach values up to 0.15 for the chosen set of benchmark models. The mixing results in modification of the Higgs boson coupling constants and therefore the model can be tested in near future by more accurate measurements of the decay and production rates of the Higgs boson.

Quite large trilinear and quartic couplings in addition to lightness of scalar sgoldstino in chosen benchmark models may also result in interesting phenomenology. In particular, one can expect new exotic Higgs decays to a pair of sgoldstinos, see for instance Figure 5. If sgoldstino decays in the detector volume, the signature is four jets (Figure 5a). It is also possible to get two jets and a missing energy if one of sgoldstinos escapes the detector volume without decay (Figure 5b). Another interesting possibility is double scalar production which looks viable due to smallness of scalar sgoldstino mass. The low energy part of the theory is, in fact, the SM extended with complex singlet scalar and studies of double scalar production have been un-

dertaken, e.g. in [85–87]. It will be interesting to perform such an analysis within the model in question to study complementarity between collider and gravitational wave experiments [88–90]. We leave study of these and similar processes for future.

## 5 Conclusions

To summarise we showed the possibility of probing the sector responsible for spontaneous supersymmetry breaking using gravitational wave signal from first order EWPT. Namely, we found that in the model with low scale supersymmetry breaking whose low energy effective theory contains, apart from the SM particles, the chiral goldstino supermultiplet, there is a region in model parameter space where the EWPT can be of the first order. Using the packages `PhaseTracer` and `FindBounce` we have found several benchmark points in the model parameter space that admit the first-order EWPT at temperatures  $T \approx 60 - 140$  GeV. For these points we have estimated the energy spectra of gravitational waves produced during the electroweak phase transition. The gravitational wave signal turns out to be of the level accessible for LISA and the proposed experiments like BBO, DECIGO and Ultimate DECIGO. We have checked the validity of perturbative description of the scalar sector at least up to the supersymmetry breaking scale, where the model naturally must be completed with the sector responsible for the supersymmetry breaking. It justifies our description of EWPT with the effective scalar potential, which parameters can be probed at Large Hadron Collider upon performing searches for light sgoldstinos.

## Acknowledgements

The work is supported by the Russian Science Foundation RSF grant 21-12-00379. The work of EK was supported by the grant of “BASIS” Foundation no. 21-2-10-37-1.

## A One-loop renormalization group equations

The one-loop equations for running coupling constants  $g_1, g_2, g_3$  of SM gauge groups  $U(1), SU(2), SU(3)$  and top quark Yukawa constant  $y_t$  read [91, 92]

$$Q \frac{\partial g_1}{\partial Q} = \frac{41g_1^3}{96\pi^2}, \quad Q \frac{\partial g_2}{\partial Q} = -\frac{19g_2^3}{96\pi^2}, \quad Q \frac{\partial g_3}{\partial Q} = -\frac{7g_3^3}{16\pi^2}, \quad (\text{A.1})$$

$$Q \frac{\partial y_t}{\partial Q} = \frac{1}{16\pi^2} \left[ \frac{9}{2}y_t^3 - 8g_3^2y_t - \frac{9}{4}g_2^2y_t - \frac{17}{12}g_1^2y_t \right]. \quad (\text{A.2})$$

The one-loop  $\beta$ -functions for dimensionless coupling constants are

$$Q \frac{\partial \lambda_1}{\partial Q} = \frac{1}{16\pi^2} \left( 24\lambda_1^2 + \frac{1}{2}\lambda_{hs}^2 + \frac{1}{2}\lambda_{hp}^2 + 12\lambda_1 y_t^2 - 3\lambda_1 g_1^2 - 9\lambda_1 g_2^2 - 6y_t^4 + \frac{3}{8}(g_1^4 + 3g_2^4 + 2g_1^2 g_2^2) \right), \quad (\text{A.3})$$

$$Q \frac{\partial \lambda_{hs}}{\partial Q} = \frac{1}{16\pi^2} \left( 12\lambda_1 \lambda_{hs} + 6\lambda_{hs} \lambda_s + \lambda_{hp} \lambda_{sp} + 4\lambda_{hs}^2 + \lambda_{hs} \left( 6y_t^2 - \frac{3}{2}g_1^2 - \frac{9}{2}g_2^2 \right) \right), \quad (\text{A.4})$$

$$Q \frac{\partial \lambda_{hp}}{\partial Q} = \frac{1}{16\pi^2} \left( 12\lambda_1 \lambda_{hp} + 6\lambda_{hp} \lambda_p + \lambda_{hs} \lambda_{sp} + 4\lambda_{hp}^2 + \lambda_{hp} \left( 6y_t^2 - \frac{3}{2}g_1^2 - \frac{9}{2}g_2^2 \right) \right), \quad (\text{A.5})$$

$$Q \frac{\partial \lambda_s}{\partial Q} = \frac{1}{16\pi^2} \left( 18\lambda_s^2 + 2\lambda_{hs}^2 + \frac{1}{2}\lambda_{sp}^2 \right), \quad (\text{A.6})$$

$$Q \frac{\partial \lambda_p}{\partial Q} = \frac{1}{16\pi^2} \left( 18\lambda_p^2 + 2\lambda_{hp}^2 + \frac{1}{2}\lambda_{sp}^2 \right), \quad (\text{A.7})$$

$$Q \frac{\partial \lambda_{sp}}{\partial Q} = \frac{1}{16\pi^2} (6\lambda_s \lambda_{sp} + 6\lambda_p \lambda_{sp} + 4\lambda_{hs} \lambda_{hp} + 4\lambda_{sp}^2). \quad (\text{A.8})$$

This result is in agreement with the renormalization group equations in [93], where the model with a Higgs boson and one new scalar is studied.

It is known that in the SM at high energies  $Q \sim 10^{10}$  GeV the Higgs boson self-coupling constant becomes negative [94]. The SM calculation of its evolution in the one-loop approximation gives the same scale  $Q$  value about  $10^8$  GeV (see figure 8 in [95]). Let us note that the second and third terms in (A.3) (diagrams with scalar and pseudoscalar sgoldstinos in the loop) increase  $\lambda_1$  and keep its value positive at higher energies up to the scale of Landau pole. For phase transitions considered in this paper the coupling constants have pole at the scales of order  $10^8 - 10^9$  GeV. We expect that deriving renormalization group equations in two loops and taking into account the input of superpartners since the 10 TeV scale moves the pole to higher energies.

The equations for coupling constants  $\mu_i$  and mass parameters  $\widetilde{M}_1^2, M_s^2, M_p^2$  read

$$Q \frac{\partial \mu_1}{\partial Q} = \frac{1}{16\pi^2} \left( 12\lambda_1 \mu_1 + 4\lambda_{hs} \mu_1 + \lambda_{hs} \mu_s + \lambda_{hp} \mu_{sp} + \mu_1 \left( 6y_t^2 - \frac{3}{2}g_1^2 - \frac{9}{2}g_2^2 \right) \right), \quad (\text{A.9})$$

$$Q \frac{\partial \mu_s}{\partial Q} = \frac{1}{16\pi^2} (18\lambda_s \mu_s + 3\lambda_{sp} \mu_{sp} + 12\lambda_{hs} \mu_1), \quad (\text{A.10})$$

$$Q \frac{\partial \mu_{sp}}{\partial Q} = \frac{1}{16\pi^2} (6\lambda_p \mu_{sp} + 4\lambda_{sp} \mu_{sp} + \lambda_{sp} \mu_s + 4\lambda_{hp} \mu_1). \quad (\text{A.11})$$

$$Q \frac{\partial \widetilde{M}_1^2}{\partial Q} = \frac{1}{16\pi^2} \left( 12\lambda_1 \widetilde{M}_1^2 - \lambda_{hs} M_s^2 - \lambda_{hp} M_p^2 - 2\mu_1^2 + \widetilde{M}_1^2 \left( 6y_t^2 - \frac{3}{2}g_1^2 - \frac{9}{2}g_2^2 \right) \right), \quad (\text{A.12})$$



$$Q \frac{\partial M_s^2}{\partial Q} = \frac{1}{16\pi^2} \left( 6\lambda_s M_s^2 + \lambda_{sp} M_p^2 - 4\lambda_{hs} \widetilde{M}_1^2 + \mu_s^2 + \mu_{sp}^2 + 4\mu_1^2 \right), \quad (\text{A.13})$$

$$Q \frac{\partial M_p^2}{\partial Q} = \frac{1}{16\pi^2} \left( 6\lambda_p M_p^2 + \lambda_{sp} M_s^2 - 4\lambda_{hp} \widetilde{M}_1^2 + 2\mu_{sp}^2 \right). \quad (\text{A.14})$$

These equations can be verified by comparison with one-loop  $\beta$ -functions and anomalous dimensions in [96], [97].

## References

- [1] H. P. Nilles, *Supersymmetry, Supergravity and Particle Physics*, *Phys. Rept.* **110** (1984) 1.
- [2] H. E. Haber and G. L. Kane, *The Search for Supersymmetry: Probing Physics Beyond the Standard Model*, *Phys. Rept.* **117** (1985) 75.
- [3] *Public results of the ATLAS experiment: supersymmetry searches*, <https://twiki.cern.ch/twiki/bin/view/AtlasPublic/SupersymmetryPublicResults>
- [4] *CMS Supersymmetry Physics Results*, <https://twiki.cern.ch/twiki/bin/view/CMSPublic/PhysicsResultsSUS>
- [5] D. V. Volkov and V. P. Akulov, *Is the Neutrino a Goldstone Particle?*, *Phys. Lett. B* **46** (1973) 109.
- [6] E. Cremmer, B. Julia, J. Scherk, P. van Nieuwenhuizen, S. Ferrara and L. Girardello, *Super-higgs effect in supergravity with general scalar interactions*, *Phys. Lett. B* **79** (1978) 231.
- [7] J. R. Ellis, K. Enqvist and D. V. Nanopoulos, *A Very Light Gravitino in a No Scale Model*, *Phys. Lett. B* **147** (1984) 99.
- [8] J. R. Ellis, K. Enqvist and D. V. Nanopoulos, *NONCOMPACT SUPERGRAVITY SOLVES PROBLEMS*, *Phys. Lett. B* **151** (1985) 357.
- [9] G. F. Giudice and R. Rattazzi, *Theories with gauge mediated supersymmetry breaking*, *Phys. Rept.* **322** (1999) 419 [arXiv:hep-ph/9801271 [hep-ph]].
- [10] S. L. Dubovsky, D. S. Gorbunov and S. V. Troitsky, *Gauge mechanism of mediation of supersymmetry breaking*, *Phys. Usp.* **42** (1999) 623 [arXiv:hep-ph/9905466 [hep-ph]].
- [11] A. Brignole, F. Feruglio and F. Zwirner, *Aspects of spontaneously broken  $N=1$  global supersymmetry in the presence of gauge interactions*, *Nucl. Phys. B* **501** (1997) 332 [arXiv:hep-ph/9703286 [hep-ph]].
- [12] A. Brignole, J. A. Casas, J. R. Espinosa and I. Navarro, *Low scale supersymmetry breaking: Effective description, electroweak breaking and phenomenology*, *Nucl. Phys. B* **666** (2003) 105 [arXiv:hep-ph/0301121 [hep-ph]].
- [13] A. Brignole and A. Rossi, *Flavor nonconservation in goldstino interactions*, *Nucl. Phys. B* **587** (2000) 3 [arXiv:hep-ph/0006036 [hep-ph]].

- [14] E. Perazzi, G. Ridolfi and F. Zwirner, *Signatures of massive sgoldstinos at  $e^+e^-$  colliders*, *Nucl. Phys. B* **574** (2000) 3 [arXiv:hep-ph/0001025 [hep-ph]].
- [15] E. Perazzi, G. Ridolfi and F. Zwirner, *Signatures of massive sgoldstinos at hadron colliders*, *Nucl. Phys. B* **590** (2000) 287 [arXiv:hep-ph/0005076 [hep-ph]].
- [16] D. S. Gorbunov and V. A. Rubakov, *Kaon physics with light sgoldstinos and parity conservation*, *Phys. Rev. D* **64** (2001) 054008 [arXiv:hep-ph/0012033 [hep-ph]].
- [17] D. Gorbunov, V. Ilyin and B. Mele, *Sgoldstino events in top decays at LHC*, *Phys. Lett. B* **502** (2001) 181 [arXiv:hep-ph/0012150 [hep-ph]].
- [18] D. S. Gorbunov and N. V. Krasnikov, *Prospects for sgoldstino search at the LHC*, *JHEP* **07** (2002) 043 [arXiv:hep-ph/0203078 [hep-ph]].
- [19] S. V. Demidov and D. S. Gorbunov, *LHC prospects in searches for neutral scalars in  $pp \rightarrow \gamma\gamma + \text{jet}$ : SM Higgs boson, radion, sgoldstino*, *Phys. Atom. Nucl.* **69** (2006) 712 [arXiv:hep-ph/0405213 [hep-ph]].
- [20] E. Dudas, C. Petersson and P. Tziveloglou, *Low Scale Supersymmetry Breaking and its LHC Signatures*, *Nucl. Phys. B* **870** (2013) 353 [arXiv:1211.5609 [hep-ph]].
- [21] S. V. Demidov and I. V. Sobolev, *Lepton flavor-violating decays of the Higgs boson from sgoldstino mixing*, *JHEP* **08** (2016) 030 [arXiv:1605.08220 [hep-ph]].
- [22] C. Petersson and A. Romagnoni, *The MSSM Higgs Sector with a Dynamical Goldstino Supermultiplet*, *JHEP* **02** (2012) 142 [arXiv:1111.3368 [hep-ph]].
- [23] K. O. Astapov and S. V. Demidov, *Sgoldstino-Higgs mixing in models with low-scale supersymmetry breaking*, *JHEP* **01** (2015) 136 [arXiv:1411.6222 [hep-ph]].
- [24] S. Demidov, D. Gorbunov and E. Kriukova, *Sgoldstino signature in  $hh$ ,  $W^+W^-$  and  $ZZ$  spectra at the LHC*, *JHEP* **05** (2020) 092 [arXiv:2003.07388 [hep-ph]].
- [25] S. Profumo, M. J. Ramsey-Musolf and G. Shaughnessy, *Singlet Higgs phenomenology and the electroweak phase transition*, *JHEP* **08** (2007) 010 [arXiv:0705.2425 [hep-ph]].
- [26] J. R. Espinosa, T. Konstandin and F. Riva, *Strong Electroweak Phase Transitions in the Standard Model with a Singlet*, *Nucl. Phys. B* **854** (2012) 592 [arXiv:1107.5441 [hep-ph]].
- [27] J. M. Cline and K. Kainulainen, *Electroweak baryogenesis and dark matter from a singlet Higgs*, *JCAP* **01** (2013) 012 [arXiv:1210.4196 [hep-ph]].
- [28] S. Profumo, M. J. Ramsey-Musolf, C. L. Wainwright and P. Winslow, *Singlet-catalyzed electroweak phase transitions and precision Higgs boson studies*, *Phys. Rev. D* **91** (2015) no.3, 035018 [arXiv:1407.5342 [hep-ph]].
- [29] M. Jiang, L. Bian, W. Huang and J. Shu, *Impact of a complex singlet: Electroweak baryogenesis and dark matter*, *Phys. Rev. D* **93** (2016) no.6, 065032 [arXiv:1502.07574 [hep-ph]].

- [30] G. Kurup and M. Perelstein, *Dynamics of Electroweak Phase Transition In Singlet-Scalar Extension of the Standard Model*, *Phys. Rev. D* **96** (2017) no.1, 015036 [arXiv:1704.03381 [hep-ph]].
- [31] S. V. Demidov, D. S. Gorbunov and D. V. Kirpichnikov, *Gravitational waves from phase transition in split NMSSM*, *Phys. Lett. B* **779** (2018) 191 [arXiv:1712.00087 [hep-ph]].
- [32] O. Gould, J. Kozaczuk, L. Niemi, M. J. Ramsey-Musolf, T. V. I. Tenkanen and D. J. Weir, *Nonperturbative analysis of the gravitational waves from a first-order electroweak phase transition*, *Phys. Rev. D* **100** (2019) no.11, 115024 [arXiv:1903.11604 [hep-ph]].
- [33] V. A. Kuzmin, V. A. Rubakov and M. E. Shaposhnikov, *On the Anomalous Electroweak Baryon Number Nonconservation in the Early Universe*, *Phys. Lett. B* **155** (1985) 36.
- [34] D. E. Morrissey and M. J. Ramsey-Musolf, *Electroweak baryogenesis*, *New J. Phys.* **14** (2012) 125003 [arXiv:1206.2942 [hep-ph]].
- [35] M. Kamionkowski, A. Kosowsky and M. S. Turner, *Gravitational radiation from first order phase transitions*, *Phys. Rev. D* **49** (1994) 2837 [arXiv:astro-ph/9310044 [astro-ph]].
- [36] R. Apreda, M. Maggiore, A. Nicolis and A. Riotto, *Gravitational waves from electroweak phase transitions*, *Nucl. Phys. B* **631** (2002) 342 [arXiv:gr-qc/0107033 [gr-qc]].
- [37] C. Grojean and G. Servant, *Gravitational Waves from Phase Transitions at the Electroweak Scale and Beyond*, *Phys. Rev. D* **75** (2007) 043507 [arXiv:hep-ph/0607107 [hep-ph]].
- [38] S. J. Huber and T. Konstandin, *Gravitational Wave Production by Collisions: More Bubbles*, *JCAP* **09** (2008) 022 [arXiv:0806.1828 [hep-ph]].
- [39] C. Caprini and D. G. Figueroa, *Cosmological Backgrounds of Gravitational Waves*, *Class. Quant. Grav.* **35** (2018) no.16, 163001 [arXiv:1801.04268 [astro-ph.CO]].
- [40] N. Craig, N. Levi, A. Mariotti and D. Redigolo, *Ripples in Spacetime from Broken Supersymmetry*, *JHEP* **21** (2020) 184 [arXiv:2011.13949 [hep-ph]].
- [41] K. Schmitz, *New Sensitivity Curves for Gravitational-Wave Signals from Cosmological Phase Transitions*, *JHEP* **01** (2021) 097 [arXiv:2002.04615 [hep-ph]].
- [42] D. S. Gorbunov and A. V. Semenov, *CompHEP package with light gravitino and goldstinos*, [arXiv:hep-ph/0111291 [hep-ph]].
- [43] S. R. Coleman and E. J. Weinberg, *Radiative Corrections as the Origin of Spontaneous Symmetry Breaking*, *Phys. Rev. D* **7** (1973) 1888.
- [44] C. W. Chiang and B. Q. Lu, *First-order electroweak phase transition in a complex singlet model with  $Z_3$  symmetry*, *JHEP* **07** (2020) 082 [arXiv:1912.12634 [hep-ph]].

- [45] L. Dolan and R. Jackiw, *Symmetry Behavior at Finite Temperature*, *Phys. Rev. D* **9** (1974) 3320.
- [46] M. E. Carrington, *The Effective potential at finite temperature in the Standard Model*, *Phys. Rev. D* **45** (1992) 2933.
- [47] P. B. Arnold and O. Espinosa, *The Effective potential and first order phase transitions: Beyond leading-order*, *Phys. Rev. D* **47** (1993) 3546 [erratum: *Phys. Rev. D* **50** (1994) 6662] [arXiv:hep-ph/9212235 [hep-ph]].
- [48] H. H. Patel and M. J. Ramsey-Musolf, *Baryon Washout, Electroweak Phase Transition, and Perturbation Theory*, *JHEP* **07** (2011) 029 [arXiv:1101.4665 [hep-ph]].
- [49] M. Garny and T. Konstandin, *On the gauge dependence of vacuum transitions at finite temperature*, *JHEP* **07** (2012) 189 [arXiv:1205.3392 [hep-ph]].
- [50] L. Niemi, P. Schicho and T. V. I. Tenkanen, *Singlet-assisted electroweak phase transition at two loops*, *Phys. Rev. D* **103** (2021) no.11, 115035 [arXiv:2103.07467 [hep-ph]].
- [51] D. Croon, O. Gould, P. Schicho, T. V. I. Tenkanen and G. White, *Theoretical uncertainties for cosmological first-order phase transitions*, *JHEP* **04** (2021) 055 [arXiv:2009.10080 [hep-ph]].
- [52] P. Athron, C. Balázs, A. Fowlie and Y. Zhang, *PhaseTracer: tracing cosmological phases and calculating transition properties*, *Eur. Phys. J. C* **80** (2020) no.6, 567 [arXiv:2003.02859 [hep-ph]].
- [53] A. Fowlie, *A fast C++ implementation of thermal functions*, *Comput. Phys. Commun.* **228** (2018) 264 [arXiv:1802.02720 [hep-ph]].
- [54] B. Laurent, J. M. Cline, A. Friedlander, D. M. He, K. Kainulainen and D. Tucker-Smith, *Baryogenesis and gravity waves from a UV-completed electroweak phase transition*, *Phys. Rev. D* **103** (2021) no.12, 123529 [arXiv:2102.12490 [hep-ph]].
- [55] A. D. Linde, *Fate of the False Vacuum at Finite Temperature: Theory and Applications*, *Phys. Lett. B* **100** (1981) 37.
- [56] A. D. Linde, *Decay of the False Vacuum at Finite Temperature*, *Nucl. Phys. B* **216** (1983) 421 [erratum: *Nucl. Phys. B* **223** (1983) 544].
- [57] M. Dine, R. G. Leigh, P. Y. Huet, A. D. Linde and D. A. Linde, *Towards the theory of the electroweak phase transition*, *Phys. Rev. D* **46** (1992) 550 [arXiv:hep-ph/9203203 [hep-ph]].
- [58] G. W. Anderson and L. J. Hall, *The Electroweak phase transition and baryogenesis*, *Phys. Rev. D* **45** (1992) 2685.
- [59] V. Guada, M. Nemevšek and M. Pintar, *FindBounce: Package for multi-field bounce actions*, *Comput. Phys. Commun.* **256** (2020) 107480 [arXiv:2002.00881 [hep-ph]].
- [60] C. Caprini, M. Chala, G. C. Dorsch, M. Hindmarsh, S. J. Huber, T. Konstandin,

- J. Kozaczuk, G. Nardini, J. M. No and K. Rummukainen, et al. *Detecting gravitational waves from cosmological phase transitions with LISA: an update*, *JCAP* **03** (2020) 024 [arXiv:1910.13125 [astro-ph.CO]].
- [61] M. E. Carrington and J. I. Kapusta, *Dynamics of the electroweak phase transition*, *Phys. Rev. D* **47** (1993) 5304.
- [62] G. D. Moore and T. Prokopec, *How fast can the wall move? A Study of the electroweak phase transition dynamics*, *Phys. Rev. D* **52** (1995) 7182 [arXiv:hep-ph/9506475 [hep-ph]].
- [63] T. Konstandin, G. Nardini and I. Rues, *From Boltzmann equations to steady wall velocities*, *JCAP* **09** (2014) 028 [arXiv:1407.3132 [hep-ph]].
- [64] J. Kozaczuk, *Bubble Expansion and the Viability of Singlet-Driven Electroweak Baryogenesis*, *JHEP* **10** (2015) 135 [arXiv:1506.04741 [hep-ph]].
- [65] A. Friedlander, I. Banta, J. M. Cline and D. Tucker-Smith, *Wall speed and shape in singlet-assisted strong electroweak phase transitions*, *Phys. Rev. D* **103** (2021) no.5, 055020 [arXiv:2009.14295 [hep-ph]].
- [66] C. Caprini, M. Hindmarsh, S. Huber, T. Konstandin, J. Kozaczuk, G. Nardini, J. M. No, A. Petiteau, P. Schwaller and G. Servant, et al. *Science with the space-based interferometer eLISA. II: Gravitational waves from cosmological phase transitions*, *JCAP* **04** (2016) 001 [arXiv:1512.06239 [astro-ph.CO]].
- [67] J. Ellis, M. Lewicki, J. M. No and V. Vaskonen, *Gravitational wave energy budget in strongly supercooled phase transitions*, *JCAP* **06** (2019) 024 [arXiv:1903.09642 [hep-ph]].
- [68] H. K. Guo, K. Sinha, D. Vagie and G. White, *Phase Transitions in an Expanding Universe: Stochastic Gravitational Waves in Standard and Non-Standard Histories*, *JCAP* **01** (2021) 001 [arXiv:2007.08537 [hep-ph]].
- [69] A. Ringwald, K. Saikawa and C. Tamarit, *Primordial gravitational waves in a minimal model of particle physics and cosmology*, *JCAP* **02** (2021) 046 [arXiv:2009.02050 [hep-ph]].
- [70] O. Gould and T. V. I. Tenkanen, *On the perturbative expansion at high temperature and implications for cosmological phase transitions*, *JHEP* **06** (2021) 069 [arXiv:2104.04399 [hep-ph]].
- [71] A. Brignole, F. Feruglio and F. Zwirner, *Signals of a superlight gravitino at  $e^+e^-$  colliders when the other superparticles are heavy*, *Nucl. Phys. B* **516** (1998) 13 [erratum: *Nucl. Phys. B* **555** (1999) 653] [arXiv:hep-ph/9711516 [hep-ph]].
- [72] A. Brignole, F. Feruglio, M. L. Mangano and F. Zwirner, *Signals of a superlight gravitino at hadron colliders when the other superparticles are heavy*, *Nucl. Phys. B* **526** (1998) 136 [erratum: *Nucl. Phys. B* **582** (2000) 759] [arXiv:hep-ph/9801329 [hep-ph]].

- [73] F. Maltoni, A. Martini, K. Mawatari and B. Oexl, *Signals of a superlight gravitino at the LHC*, *JHEP* **04** (2015) 021 [arXiv:1502.01637 [hep-ph]].
- [74] S. V. Demidov and I. V. Sobolev, *Low scale supersymmetry at the LHC with jet and missing energy signature*, [arXiv:1709.03830 [hep-ph]].
- [75] J. S. Kim, S. Pokorski, K. Rolbiecki and K. Sakurai, *Gravitino vs Neutralino LSP at the LHC*, *JHEP* **09** (2019) 082 [arXiv:1905.05648 [hep-ph]].
- [76] A. M. Sirunyan et al. [CMS], *Search for supersymmetry in final states with photons and missing transverse momentum in proton-proton collisions at 13 TeV*, *JHEP* **06** (2019) 143 [arXiv:1903.07070 [hep-ex]].
- [77] A. M. Sirunyan et al. [CMS], *Search for supersymmetry in events with a photon, jets, b-jets, and missing transverse momentum in proton-proton collisions at 13 TeV*, *Eur. Phys. J. C* **79** (2019) no.5, 444 [arXiv:1901.06726 [hep-ex]].
- [78] A. M. Sirunyan et al. [CMS], *Inclusive search for supersymmetry in pp collisions at  $\sqrt{s} = 13$  TeV using razor variables and boosted object identification in zero and one lepton final states*, *JHEP* **03** (2019) 031 [arXiv:1812.06302 [hep-ex]].
- [79] A. M. Sirunyan et al. [CMS], *Search for supersymmetry in events with a photon, a lepton, and missing transverse momentum in proton-proton collisions at  $\sqrt{s} = 13$  TeV*, *JHEP* **01** (2019) 154 [arXiv:1812.04066 [hep-ex]].
- [80] M. Aaboud et al. [ATLAS], *Search for supersymmetry in events with four or more leptons in  $\sqrt{s} = 13$  TeV pp collisions with ATLAS*, *Phys. Rev. D* **98** (2018) no.3, 032009 [arXiv:1804.03602 [hep-ex]].
- [81] M. Aaboud et al. [ATLAS], *Search for photonic signatures of gauge-mediated supersymmetry in 13 TeV pp collisions with the ATLAS detector*, *Phys. Rev. D* **97** (2018) no.9, 092006 [arXiv:1802.03158 [hep-ex]].
- [82] M. Aaboud et al. [ATLAS], *Search for squarks and gluinos in final states with hadronically decaying  $\tau$ -leptons, jets, and missing transverse momentum using pp collisions at  $\sqrt{s} = 13$  TeV with the ATLAS detector*, *Phys. Rev. D* **99** (2019) no.1, 012009 [arXiv:1808.06358 [hep-ex]].
- [83] M. J. Ramsey-Musolf, *The electroweak phase transition: a collider target*, *JHEP* **09** (2020) 179 [arXiv:1912.07189 [hep-ph]].
- [84] M. Asano and R. Garani, *Sgoldstino search at the LHC*, [arXiv:1701.00829 [hep-ph]].
- [85] C. Y. Chen, J. Kozaczuk and I. M. Lewis, *Non-resonant Collider Signatures of a Singlet-Driven Electroweak Phase Transition*, *JHEP* **08** (2017) 096 [arXiv:1704.05844 [hep-ph]].
- [86] M. Carena, Z. Liu and M. Riembau, *Probing the electroweak phase transition via enhanced di-Higgs boson production*, *Phys. Rev. D* **97** (2018) no.9, 095032 [arXiv:1801.00794 [hep-ph]].
- [87] T. Robens, T. Stefaniak and J. Wittbrodt, *Two-real-scalar-singlet extension of the*

- SM: LHC phenomenology and benchmark scenarios*, *Eur. Phys. J. C* **80** (2020) no.2, 151 [arXiv:1908.08554 [hep-ph]].
- [88] A. Alves, T. Ghosh, H. K. Guo, K. Sinha and D. Vagie, *Collider and Gravitational Wave Complementarity in Exploring the Singlet Extension of the Standard Model*, *JHEP* **04** (2019) 052 [arXiv:1812.09333 [hep-ph]].
- [89] A. Alves, D. Gonçalves, T. Ghosh, H. K. Guo and K. Sinha, *Di-Higgs Production in the 4b Channel and Gravitational Wave Complementarity*, *JHEP* **03** (2020) 053 [arXiv:1909.05268 [hep-ph]].
- [90] A. Papaefstathiou and G. White, *The electro-weak phase transition at colliders: confronting theoretical uncertainties and complementary channels*, *JHEP* **05** (2021) 099 [arXiv:2010.00597 [hep-ph]].
- [91] M. x. Luo and Y. Xiao, *Two loop renormalization group equations in the standard model*, *Phys. Rev. Lett.* **90** (2003) 011601 [arXiv:hep-ph/0207271 [hep-ph]].
- [92] M. Shaposhnikov and C. Wetterich, *Asymptotic safety of gravity and the Higgs boson mass*, *Phys. Lett. B* **683** (2010) 196-200 [arXiv:0912.0208 [hep-th]].
- [93] K. Kainulainen, K. Tuominen and V. Vaskonen, *Self-interacting dark matter and cosmology of a light scalar mediator*, *Phys. Rev. D* **93** (2016) no.1, 015016 [erratum: *Phys. Rev. D* **95** (2017) no.7, 079901] [arXiv:1507.04931 [hep-ph]].
- [94] G. Degrandi, S. Di Vita, J. Elias-Miro, J. R. Espinosa, G. F. Giudice, G. Isidori and A. Strumia, *Higgs mass and vacuum stability in the Standard Model at NNLO*, *JHEP* **08** (2012) 098 [arXiv:1205.6497 [hep-ph]].
- [95] J. Brod and Z. Polonsky, *Two-loop Beta Function for Complex Scalar Electroweak Multiplets*, *JHEP* **09** (2020) 158 [arXiv:2007.13755 [hep-ph]].
- [96] M. Holthausen, K. S. Lim and M. Lindner, *Planck scale Boundary Conditions and the Higgs Mass*, *JHEP* **02** (2012) 037 [arXiv:1112.2415 [hep-ph]].
- [97] P. Ghorbani, *On Vacuum Stability in Real Singlet Scalar Extension of the Standard Model*, *Nucl. Phys. B* **971** (2021) 115533 [arXiv:2104.09542 [hep-ph]].